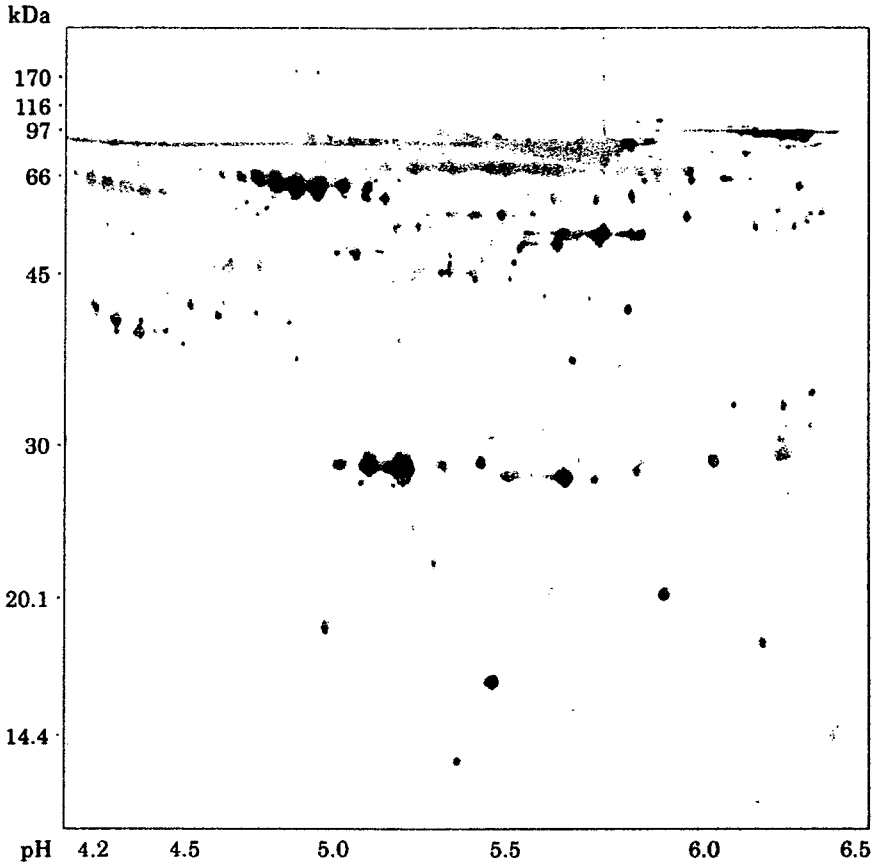

Figure 1. Serum protein patterns on a 2-DE gel (12.5%) after the removal of immunoglobulin. The 2-DE running conditions are described in the text. Protein (300 μg) was loaded onto the IEF gel strip (pH 4–7). Following 2-DE separation, the protein spots were visualized by silver staining and were numbered using the PDQuest software. A representative gel image is shown.

Table 1. Profiles of patients. Eight cases infected with hepatitis virus with HCC were enrolled in this analysis. Second column is TNM staging and max size of hepatocellular carcinoma(cm). TNM is tumor staging system, which uses three criteria to judge the stage of the cancer – primary tumor(T), rigional lymph nodes(N), and distant metastasis(M) – stage I through IV. AFP, L3 and DCP are HCC tumor markers, which are often clinically used. L3 fraction is a fucosylated AFP subtype and more specific for HCC than AFP. If TAE was done, it was stated in the last column

	cases	TNM/radius	changes by the treatment			
			AFP (IU/L)	L3 (%)	DCP (IU/L)	
1.	70F C-LC	II/ϕ 1,4 cm	7 ⇒ 7	N.D.	18 ⇒ 16	
2.	81M C-CH	I/ϕ 1,2 cm	32 ⇒ 29	2.0 ⇒ 0.5	13 ⇒ 15	
3.	64M C-CH	II/ϕ 2,1 cm	11 ⇒ 12	0.5 ⇒ 0.5	13 ⇒ 14	
4.	56F B-LC	II/ϕ 3,0 cm	162 ⇒ 55	43.3 ⇒ 33.2	10 ⇒ 10	TAE(+)
5.	74F C-LC	III/ϕ 2,9 cm	8855 ⇒ 912	5.2 ⇒ 7.0	134 ⇒ 16	TAE(+)
6.	55F B-CH	II/ϕ 3,2 cm	7 ⇒ 5	N.D.	59 ⇒ 18	TAE(+)
7.	58M C-LC	I/ϕ 1,5 cm	195 ⇒ 132	12.0 ⇒ 5.3	12 ⇒ 13	
8.	64F C-CH	II/ϕ 3,0 cm	1375 ⇒ 108	1.7 ⇒ 2.4	24 ⇒ 13	TAE(+)

TAE: transarterial embolization, N.D.: not detected

In order to ensure reproducibility, the 2-DE pattern of each patient serum sample was analyzed in two separate experiments. The image analysis showed that these 2-DE maps were similar, as shown in Fig. 1. Using the PDQuest image analysis software, 1133 spots were resolved on the 2-DE gels.

After excluding spots with intensities that varied by over 2 SD in duplicate gels (Fig. 2), hierarchical clustering

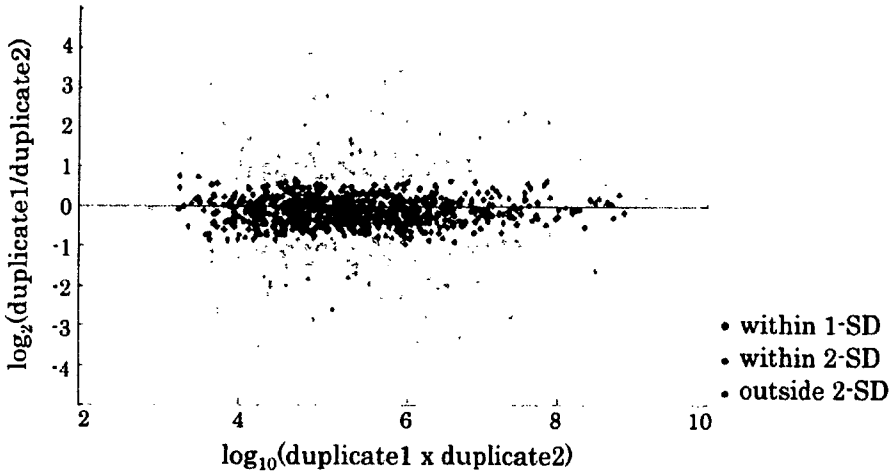

Figure 2. Reproducibility of 2-DE-based protein spot quantification. The spot intensity-dependent SD was calculated based on the ratio-intensity plot, using the data from duplicate experiments. Protein spots with intensities that varied by >2 × SD between experiments were eliminated from the subsequent analysis.

was performed with the remaining 812 spots. As shown in Fig. 3A, the unsupervised clustering analysis demonstrated that each pair of samples before and after RFA treatment lined up side by side, except in case 2, which means that the treatment did not produce any drastic change in the protein abundance in common across the eight patients. We may have missed subtle changes that could be associated with the tumor. Therefore, we divided the serum samples into two groups, *i.e.*, before and after treatment, and performed supervised clustering analysis to discover proteins expressed differentially with the treatment. Of 812 protein spots, 88 protein spots were selected as changing significantly in this analysis (Fig. 3B).

3.2 Protein identification of spots

The 88 protein spots shown in Fig. 3B were subjected to in-gel trypsin digestion and MS, and 45 protein spots (51%) were identified. Many of these identified spots represented PTM variants; they were collapsed into 11 distinct proteins after homology and similarity searches to eliminate redundant protein annotations. Although 15 protein spots are shown in Table 2 and Fig. 3B (asterisks), they still contain PTM variants. The remaining differential protein spots were not identified at this point, because the spot intensities were too faint to obtain sufficient amounts of tryptic peptide for protein identification. Several spots were identified by MALDI-TOF/TOF analysis.

The levels of four proteins were decreased after RFA: PRO1708/PRO2044 (the C-terminal fragment of albumin), pro-apolipoprotein, α2-HS glycoprotein (AHSG), and apolipoprotein A-IV precursor (Table 2 and Fig. 4A). The levels of seven proteins were increased after treatment: leucine-rich α2-glycoprotein, α1-antitrypsin, macroglobulin α2, haptoglobin (precursor), serum paraoxonase, complement C3 precursor, and C4A (Fig. 4B).

3.3 Western blotting with the anti-AHSG antibody

The expression of AHSG was confirmed by Western blot analysis with the anti-AHSG antibody. Paired sera from the patients were dissolved in SDS-PAGE gel buffer and blotted onto PVDF membranes. As shown in Fig. 5, the AHSG protein level was decreased after RFA treatment in three of six patients.

4 Discussion

Chronic infection with HBV or HCV is a significant risk factor for the development of HCC [18, 19]. The monitoring of disease progression and the prediction of outcome currently depend on a combination of physical and serological assessments. Unfortunately, these methods often lack the sensitivity required to detect HCC at an early stage, when therapeutic options are the most effective, especially when all three of the HCC markers AFP, L3 (fucosylated fraction of AFP), and DCP, are within normal ranges. There is a very real need for the discovery of markers that can detect the disease at an earlier stage in a higher proportion of patients and that are suitable for screening populations known to be at high risk for the development of HCC.

In the search for new biomarkers, several groups have analyzed differences in the levels of RNA expressed in normal and tumor-derived liver tissues [21–24] or in cultured cells [22, 25–27]. Similarly, some groups have studied differences in the protein profiles, or proteomes, of normal and tumor-derived liver tissues, cell lines, and serum [8, 9]. These studies have provided new insights into tumor carcinogenesis. For the discovery of disease progression markers that can be used for HCC patient screening, it is desirable to uncover changes in specific gene products that can be found in samples, such as serum, that are easily collected from patients.

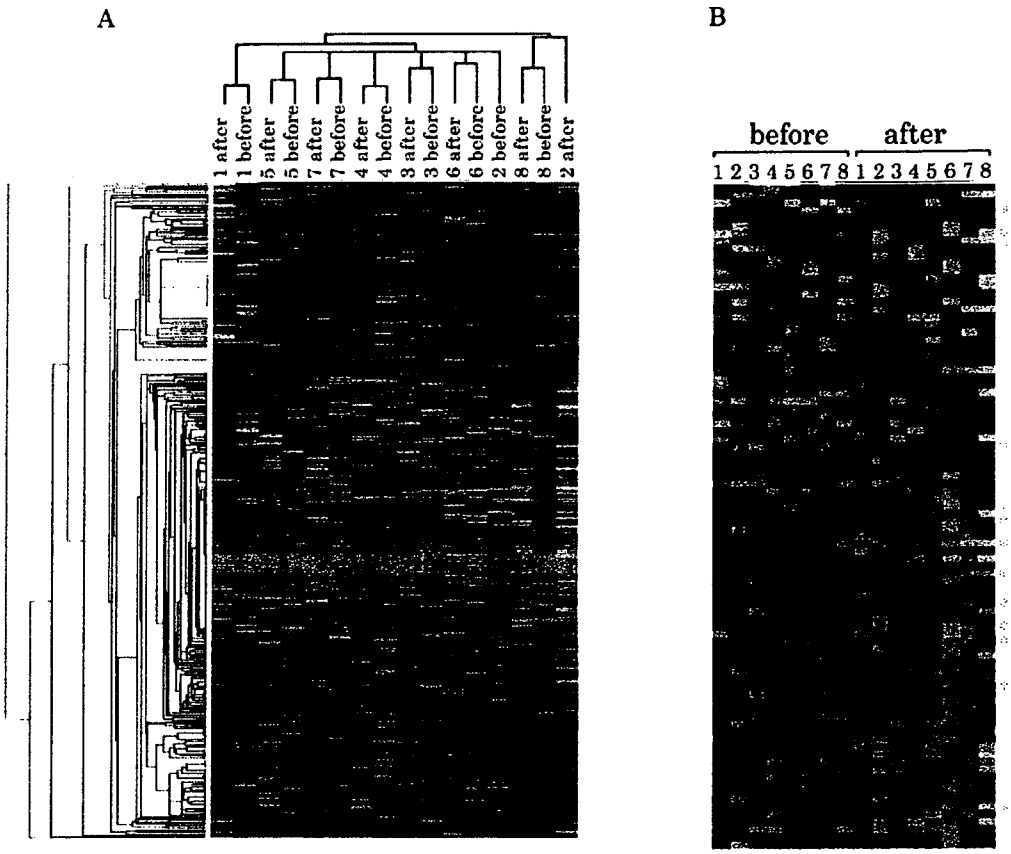

Figure 3. Hierarchical clustering analysis of serum protein spots. (A) Unsupervised clustering of eight cases and 812 spots. (B) Eighty-eight protein spots that were expressed differentially before and after treatment for HCC were selected in the supervised clustering analysis. Of these, 45 protein spots were identified using MS. The 15 spots indicated by asterisks (also listed in Table 2) still contain variants modified post-translationally, and the final number of proteins that changed with treatment is 11. Gray: missing value.

Table 2. Identified proteins by mass spectrometry. 2-DE gel images were analyzed by PDQuest software and detected spots were numbered (Spot no.). The values of score, M_r and p*I* are indicated in MASCOT MS/MS Ion search. The ratio between before and after treatment is indicated as Ratio (before/after). The scaling factor of the spot intensity used in PDQuest software is PPM (parts per million) and Mean and SE (standard error) of each spot was calcurated. Corrected p values <0.05 were considered to be significant. Right panel is the heat map extracted from the Fig. 3 of each protein. The line order is as same as Table 2.

Spot no.	Protein identified	Accesion no.	Score	Ratio (before/after)	Mr (kDa)	pI	Mean	SE
9010	PRO1708 /PRO2044	gi|7959791 /gi6650826	62	3.65	29.2	7.0	2467	433
3115	proapolipoprotein	gi|178775	124	2.08	28.9	5.5	1112	251
638	alpha2-HS glycoprotein	gi|2521981	180	1.44	35.6	5.2	5882	629
1605	alpha2-HS glycoprotein	gi|2521981	30	1.39	35.6	5.2	190	34
3401	apolipoprotein A-IV precursor	gi|178779	109	2.33	43.4	5.2	990	205
501	leucine-rich α-2-glycoprotein	gi|72059	63	0.44	34.3	5.7	1365	209
504	leucine-rich α-2-glycoprotein	gi|16418467	37	0.54	38.2	6.5	1520	169
2808	alpha-1-antitrypsin	gi|177831	68	0.52	46.7	5.4	1145	196
8801	macroglobulin α2	gi|224053	115	0.61	160.7	6.0	323	32
6003	haptoglobin Hp2	gi|223976	154	0.55	41.7	6.2	5235	1036
2414	haptoglobin precursor	gi|306882	106	0.52	45.2	6.1	2966	2349
1507	serum paraoxonase	gi|130675	112	0.41	39.7	5.1	2470	576
1514	serum paraoxonase	gi|130675	112	0.43	39.7	5.1	6798	1798
1412	complement C3 precursor	gi|4557385	129	0.41	187.1	6.0	459	231
4207	complement C4A	gi|443671	158	0.54	193.5	6.8	525	97

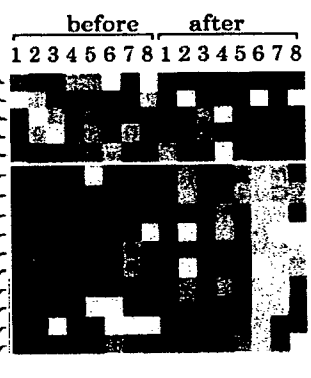

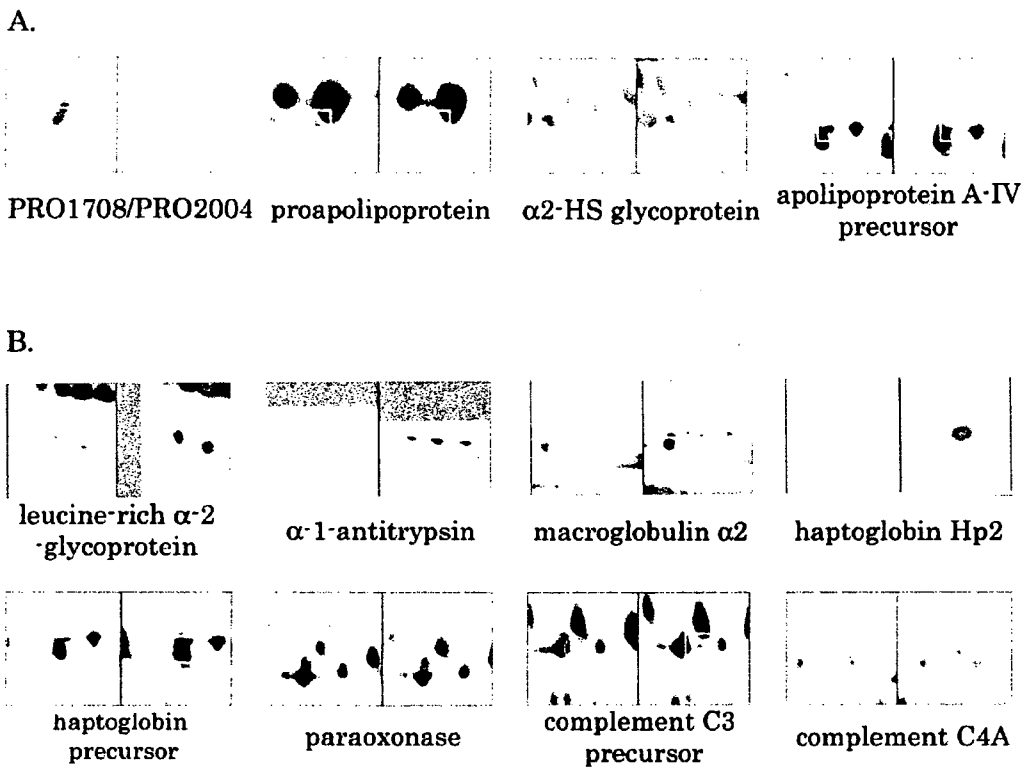

Figure 4. Identification of spots that exhibited changed levels in response to HCC treatment. (A) Identified spots with decreased levels after treatment. PRO1708/PRO2204 is the C-terminal fragment of albumin. (B) Identified spots with increased levels after treatment. Each spot is enclosed in a square, and representative gels images are shown.

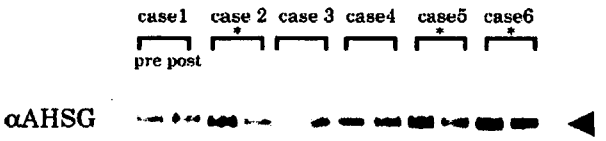

Figure 5. Western blot using the anti-AHSG antibody. Sera were run on a 10–20% gel. The Western blot shows that, in cases 2, 5, and 6, the levels of AHSG were higher before treatment than after treatment.

Steel *et al.* [9] properly dealt with the variability between individuals by combining an equal mass of total serum protein from individuals to form a composite sample for each of the four groups and by comparing the composite 2-DE gels of the four groups. As shown in Table 1, we lacked sufficient samples to detect significant differences, and the patients had different etiological backgrounds. We tried to minimize the variance between individuals by comparing paired gels derived from the same patient's serum. The constituents of serum after treatment must be the same as those before treatment, except for tumor-associated proteins or the consequences of treatment, in order to compare serum samples from the same patient. The timing of serum collection after treatment is important for comparative analysis, and we collected the post-treatment sera 1 wk after treatment, at the time of discharge from hospital. We considered this period of time reasonable in the clinical setting.

As described in Section 2, we collected serum samples before and after HCC treatment. At the time of discharge, the transaminases (ALT/AST) were unchanged or slightly upregulated from before treatment (the ratios of after/before were between 0.9 and 2; data not shown). It was not practical to wait for 1 month for all the serological parameters to stabilize and the tumor makers to decrease markedly in some cases, as shown in Table 1. Thus we considered 1 wk a reasonable interval and carefully continued our analyses, introducing a statistical analysis to eliminate artifactual errors.

In this study, we identified four proteins that had decreased levels following HCC treatment (Table 2). None of these proteins has been reported to be associated with liver cancer. Apolipoprotein A-IV (precursor) is synthesized primarily in the intestine [28, 29] and is secreted in the plasma; because its expression is suppressed in the sera of HBV-infected individuals, it is assumed to be an indicator of HBV infection [9]. AHSG, which is also known as human fetuin, is a liver secretory glycoprotein found at high levels in the serum and mineralized bone. This protein has the char-

acteristics of a negative acute-phase protein, in that the serum concentrations decrease significantly after major surgical procedures, trauma, burns, and severe inflammation. Western blotting with the anti-AHSG antibody confirmed that the serum level of AHSG was decreased by HCC treatment (Fig. 5). The protein with the most significant change in abundance was PRO1708/PRO2044 (Table 2). This protein is the C-terminal part of albumin. However, it was spotted in a very different location from albumin (the M_r and p*I* values of PRO1708/PRO2044 are 29 kDa and 7.6, respectively, whereas those of albumin are 69 kDa and 6.0 in 2-DE gels). We postulated that the partial fragment had a special physiological meaning; therefore, we used PRO1708/PRO2044 instead of a fragment of albumin in the text and table.

PRO1708/PRO2044 and AHSG were upregulated in the sera of HCC patients, as compared with levels in HCC-eradicated sera. Although the levels of AHSG may fluctuate as a result of liver damage or inflammation, it is not clear why the levels of the other proteins decrease after treatment. These results suggest roles for these proteins in HCC, but further confirmatory studies are necessary.

The levels of seven different proteins were elevated after HCC treatment. The increases in the levels of these proteins may be attributable to acute stress reactions or leakage from damaged liver tissues. Serum haptoglobin levels are widely used to study various liver diseases and are reported to be linked to liver damage in HBV liver infection [9]. Liver injury caused by RFA treatment may have increased the intensities of the spots. As a powerful inhibitor of apoptosis and caspase activation, α1-antitrypsin inhibits many of the proteases that are released from dying cells, and thus protects normal tissues during periods of stress, such as inflammation [9]. The observed increases in the α1-antitrypsin levels of the post-treatment sera may represent self-protective responses of the liver. Although Steel *et al.* [8] found that a fragment of complement C3 was downregulated in HCC, we identified complement C3 as being upregulated after RFA treatment. This could indicate recovery of the liver, although more study is necessary.

As shown in Table 1, the types of tumor markers produced by HCC differ among patients, and neither the sensitivity nor the specificity of the three markers is satisfactory. As the sample number was small and the patients had different etiological backgrounds, the clinical significance of the proteins identified here must be explored by analyzing more cases. We propose an analytical procedure using a standard statistical algorithm [14] with carefully normalized and transformed data [13] in combination with protein identification using TOF/TOF technology.

As previously described, AFP, L3, and DCP are frequently used clinical HCC tumor markers. L3, which is a fucosylated fraction of AFP, is considered more specific than AFP for HCC. We tried to evaluate the degrees of differences in individuals around the time of treatment using these three HCC markers, but it proved too difficult. Albumin is a carrier protein for many small proteins and peptides, is one of the most abundant proteins, and has an M_r of 69 kDa and a p*I* value of 6. Different forms of modified/processed albumin appear and form multiple spots in the 2-DE gel, which leave traces that make it difficult to detect spots with a p*I* value lower than 6. AFP, the L3 fraction, and DCP are positioned in this area, and it is technically difficult to identify these proteins on gels.

In the final analysis, we identified 45 of the 812 protein spots on the 2-DE gels using MS/MS. As listed in Table 2, many of these identified spots represented PTM variants; they collapsed into 15 distinct proteins after homology and similarity searches eliminated redundant protein annotations (indicated as asterisks in Fig. 3B, and Table 2).

The technique of comparative proteomics is an effective platform for the study of cancer. The 2-DE images presented in this study will facilitate the identification of potential tumor markers and increase our understanding of the mechanisms of HCC.

This work was supported by a research grant from the Ministry of Culture, Science, and Sports. We thank Mitsuko Tsubouchi for technical assistance.

5 References

[1] Kew, M. C. *et al.*, *Sleisenger and Fordtran's Gastrointestinal and Liver Disease*, W. B. Saunders, Philadelphia 1998, pp. 1577–1602.

[2] El-Serag, H. B., Mason, A. C., Key, C., *Hepatology* 2001, *33*, 62–65.

[3] Shiina, S., Teratani, T., Obi, S., Hamamura, K. *et al.*, *Oncology* 2002, *62 Suppl 1*, 64–68.

[4] Livraghi, T., *Eur J Ultrasound* 2001, *13*, 167–176.

[5] Omata, M., Yoshida, H., Shiratori, Y., Shiina, S., *J. Gastroenterol. Hepatol.* 2002, *17 Suppl 3*, S434–S436.

[6] Wulfkuhle, J. D., Liotta, L. A., Petricoin, E. F., *Nat. Rev. Cancer* 2003, *3*, 267–275.

[7] Petricoin, E. F., Liotta, L. A., *Curr. Opin. Biotechnol.* 2004, *15*, 24–30.

[8] Steel, L. F., Shumpert, D., Trotter, M., Seeholzer, S. H. *et al.*, *Proteomics* 2003, *3*, 601–609.

[9] He, Q. Y., Lau, G. K., Zhou, Y., Yuen, S. T. *et al.*, *Proteomics* 2003, *3*, 666–674.

[10] Medzihradszky, K. F., Campbell, J. M., Baldwin, M. A., Falick, A. M. *et al.*, *Anal. Chem.* 2000, *72*, 552–558.

[11] Bienvenut, W. V., Deon, C., Pasquarello, C., Campbell, J. M. *et al.*, *Proteomics* 2002, *2*, 868–876.

[12] Blum, H., Beier, H., Gross, H. J., *Electrophoresis* 1987, *8*, 93–99.

[13] Quackenbush, J., *Nat. Genet.* 2002, *32 Suppl*, 496–501.

[14] Eisen, M. B., Spellman, P. T., Brown, P. O., Botstein, D., *Proc. Natl. Acad. Sci. U S A* 1998, *95*, 14863–14868.

[15] Katayama, H., Nagasu, T., Oda, Y., *Rapid Commun. Mass Spectrom.* 2001, *15*, 1416–1421.

[16] Bienvenut, W. V., Sanchez, J. C., Karmime, A., Rouge, V. *et al.*, *Anal. Chem.* 1999, *71*, 4800–4807.

[17] Kawakami, T., Chiba, T., Suzuki, T., Iwai, K. *et al.*, *EMBO J.* 2001, *20*, 4003–4012.

[18] Bosch, F. X., Ribes, J., Borras, J., *Semin. Liver Dis.* 1999, *19*, 271–285.

[19] Parkin, D. M., Pisani, P., Ferlay, J., *Int. J. Cancer* 1999, *80*, 827–841.

[20] Scopes, R. K., *Protein Purification: Principles and Practice*, Springer-Verlag, New York1994.

[21] Yamashita, T., Kaneko, S., Hashimoto, S., Sato, T. *et al.*, *Biochem. Biophys. Res. Commun.* 2001, *282*, 647–654.

[22] Shirota, Y., Kaneko, S., Honda, M., Kawai, H. F. *et al.*, *Hepatology* 2001, *33*, 832–840.

[23] Xu, X. R., Huang, J., Xu, Z. G., Qian, B. Z. *et al.*, *Proc. Natl. Acad. Sci. U S A* 2001, *98*, 15089–15094.

[24] Graveel, C. R., Jatkoe, T., Madore, S. J., Holt, A. L. *et al.*, *Oncogene* 2001, *20*, 2704–2712.

[25] Wirth, P. J., *Electrophoresis* 1994, *15*, 358–371.

[26] Yu, L. R., Zeng, R., Shao, X. X., Wang, N. *et al.*, *Electrophoresis* 2000, *21*, 3058–3068.

[27] Peebles, K. A., Duncan, M. W., Ruch, R. J., Malkinson, A. M., *Carcinogenesis* 2003, *24*, 651–657.

[28] Tso, P., Liu, M., Kalogeris, T. J., Thomson, A. B., *Annu. Rev. Nutr.* 2001, *21*, 231–254.

[29] Vergnes, L., Taniguchi, T., Omori, K., Zakin, M. M. *et al.*, *Biochim. Biophys. Acta.* 1997, *1348*, 299–310.

Available online at www.sciencedirect.com
SCIENCE DIRECT
Bioorganic & Medicinal Chemistry
ELSEVIER
Bioorganic & Medicinal Chemistry 14 (2006) 1437–1443

Structural basis for DNA-cleaving activity of resveratrol in the presence of Cu(II)

Kiyoshi Fukuhara,[a,*] Maki Nagakawa,[b] Ikuo Nakanishi,[c,d] Kei Ohkubo,[d] Kohei Imai,[e] Shiro Urano,[e] Shunichi Fukuzumi,[d] Toshihiko Ozawa,[c] Nobuo Ikota,[c] Masataka Mochizuki,[b] Naoki Miyata[f] and Haruhiro Okuda[a]

[a]*Division of Organic Chemistry, National Institute of Health Sciences, 1-18-1 Setagaya-ku, Tokyo 158-8501, Japan*
[b]*Division of Organic and Bioorganic Chemistry, Kyoritsu University of Pharmacy, 1-5-30 Shibakoen, Minato-ku, Tokyo 105-8512, Japan*
[c]*Redox Regulation Research Group, Research Center for Radiation Safety, National Institute of Radiological Sciences (NIRS), 4-9-1 Anagawa, Inage-ku, Chiba 263-8555, Japan*
[d]*Department of Material and Life Science, Graduate School of Engineering, Osaka University, SORST, Japan Science and Technology Agency (JST), 2-1 Yamada-oka, Suita, Osaka 565-0871, Japan*
[e]*Department of Applied Chemistry, Shibaura Institute of Technology, Minato-ku, Tokyo 108-8548, Japan*
[f]*Graduate School of Pharmaceutical Sciences, Nagoya City University, 3-1 Tanabe-dori, Mizuho-ku, Nagoya, Aichi 467-8603, Japan*

Received 31 August 2005; revised 27 September 2005; accepted 27 September 2005
Available online 24 October 2005

Abstract—Resveratrol (**1**, 3,5,4′-trihydroxy-*trans*-stilbene), a polyphenol found in grapes and other food products, is known as an antioxidant and cancer chemopreventive agent. However, **1** was shown to induce genotoxicity through a high frequency of micronucleus and sister chromatid exchange in vitro and DNA-cleaving activity in the presence of Cu(II). The present study was designed to explore the structure–activity relationship of **1** in DNA strand scission and to characterize the substrate specificity for Cu(II) and DNA binding. When pBR322DNA was incubated with **1** or its analogues differing in the number and positions of hydroxyl groups in the presence of Cu(II), the ability of 4-hydroxystilbene analogues to induce DNA strand scission is much stronger than that of 3-hydroxy analogues. The high binding affinity with both Cu(II) and DNA was also observed by 4-hydroxystilbene analogues. The reduction of Cu(II) which is essential for activation of molecular oxygen proceeded by addition of **1** to the solution of the Cu(II)–DNA complex, while such reduction was not observed with the addition of isoresveratrol, in which the 4-hydroxy group of **1** is changed to the 3-position. The results show that the 4-hydroxystilbene structure of **1** is a major determinant of generation of reactive oxygen species that was responsible for DNA strand scission.

1. Introduction

Natural polyphenols, including catechin, epicatechin, quercetin, and resveratrol, are natural antioxidants that are found in a wide range of plant species. Polyphenols inhibit the oxidation of human low-density lipoprotein (LDL),[1] which is responsible for promoting atherogenesis,[2,3] and the intake of foods and beverages that contain polyphenols may protect against atherosclerosis.[4] The polyphenol resveratrol (3,5,4′-trihydroxy-*trans*-stilbene; **1**) is found in grapes, where it serves as a phytoalexin that protects against fungal infection.[5] Although its biosynthesis is not well defined, **1** is thought to be synthesized in response to infection or injury.[6] Resveratrol **1** (Fig. 1) has some therapeutic effects that are due to its antioxidant potential and originate from the inhibition of the oxidation of human LDL and the reduced propensity of human plasma and LDL to undergo lipid peroxidation.[7,8] In addition to its antioxidant potential, it has also been reported to have a variety of anti-inflammatory, anti-platelet, and anti-carcinogenic effects.[9,10] Therefore, due to its high concentration in grape skin, the beneficial effects of the consumption of red wine at reducing the risk of cardiovascular disease have been attributed to the multiple effects of **1**.[11] Recently, **1** was shown to inhibit cellular events associated with

Keywords: Resveratrol; Polyphenol; Antioxidant; DNA oxidative damage.
* Corresponding author. Tel.: +81-3-3700-1141; fax: +81-3-3707-6950; e-mail: fukuhara@nihs.go.jp

0968-0896/$ - see front matter © 2005 Elsevier Ltd. All rights reserved.
doi:10.1016/j.bmc.2005.09.070

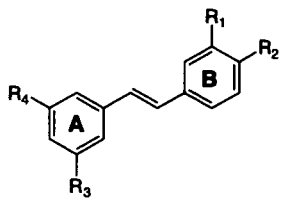

	R_1	R_2	R_3	R_4
1	H	OH	OH	OH
2	OH	H	OH	OH
3	H	H	OH	OH
4	H	OH	OH	H
5	OH	H	OH	H
6	OH	H	H	H
7	H	OH	H	H
8	OH	OH	OH	OH
9	OH	OH	OH	H
$1H_2$	H	OH	OH	OH

Figure 1. Structure of resveratrol (**1**), its analogues **2–9**, and dihydroresveratrol ($\mathbf{1H_2}$).

tumor initiation, promotion, and progression.[12] Furthermore, it has been reported that **1** has the potential to inhibit DNA polymerase and cyclooxygenase,[13] and also has a direct antiproliferative effect on human breast epithelial cells.[14] Based on its antimutagenic activity,[15,16] it has been suggested that **1** should be effective as a cancer chemopreventive agent in humans.

Meanwhile, 5-alkyl-1,3-dihydroxybenzenes (5-alkylresorcinol) have long been recognized to have potential as therapeutic agents, since natural resorcinols have a wide variety of biological activities, including fungicidal and bactericidal activities against numerous pathogens.[17] Hecht and co-workers were the first to demonstrate that 5-alkylresorcinol induced Cu(II)-dependent DNA strand scission under alkaline pH.[18] This DNA cleavage requires the initial oxygenation of the benzene nucleus, a process that occurs readily at an alkaline pH in the presence of Cu(II) and O_2. The resulting trihydroxylated benzene mediates DNA cleavage in a reaction that depends on the presence of Cu(II) and O_2. Recently, based on the similar structures of 5-alkylresorcinol and resveratrol, we suggested that **1** may be able to mediate Cu(II)-dependent DNA strand scission under neutral conditions.[19] Interestingly, DNA strand scission occurred at neutral pH, indicating that **1** can induce DNA cleavage without the oxygenation of benzene nuclei to the catechol moiety, which is a requisite intermediate in resorcinol-induced DNA cleavage. It has also been shown that DNA cleavage is more likely caused by a copper–peroxide complex as the reactive species rather than by a freely diffusible oxygen species that mediates DNA degradation by resorcinol in the presence of Cu(II). However, instead of the catechol structure, the structural feature of **1** that is effective for DNA cleavage is still unknown. To address this question, the present study was designed to explore the structure–activity relationship of synthesized hydroxystilbene derivatives (Fig. 1) in DNA strand 4 scission and also to characterize the substrate specificity for Cu(II) and DNA binding. The results show that the 4-hydroxy group of **1** is a major determinant of DNA cleaving ability and confirm that the stilbene structure is also important for this ability.

2. Result and discussion

2.1. DNA-cleaving activity

The ability of **1** and its analogues to induce DNA-cleaving activity was examined using pBR322, a supercoiled, covalently closed circular DNA (Form I), and analyzed by agarose gel electrophoresis. Consistent with the fact that Cu(II) is required for potent DNA-cleaving activity of **1**, the individual hydroxylated stilbenes induced DNA cleavage only when the reaction was carried out in the presence of Cu(II); in the absence of Cu(II), no DNA cleavage was observed (data not shown). Figure 2 shows the results of the analysis in the presence of Cu(II). Replacement of the internal double bond in the stilbene moiety by a saturated one ($\mathbf{1H_2}$) resulted in a marked reduction in potency, suggesting that the structure of stilbene is important for mediating DNA relaxation. In a series of hydroxylated stilbene analogues, Cu(II)-dependent DNA-cleaving activity was greatly affected by the number and positions of hydroxyl groups attached to the stilbene structure. For a given structural series (i.e., all 4-OH analogues: **1**, **4**, **7**; 3-OH analogues: **2**, **3**, **5**, **6**; or 3,4-(OH) analogues: **8**, **9**), the DNA-cleaving activity seemed to increase with an increase in the number of hydroxyl groups. Densitometric analysis of agarose gel indicated that the DNA-cleaving ability of **1** resulted not only in the complete conversion of substrate DNA (Form I) into open circular DNA (Form II) but also the further conversion of Form II into linear

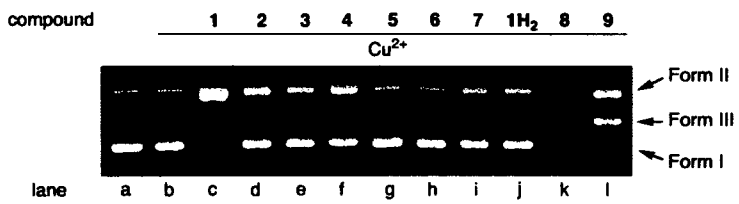

Figure 2. Gel electrophoretic analysis of single- and double-strand breaks generated in pBR322DNA with **1** or its analogues in the presence of Cu(II). Assays were performed in 50 mM sodium cacodylate buffer, pH 7.2, containing 45 μbp pBR322DNA and 10 μM of samples (lane c–l) in the presence of 10 μM Cu(II) (lane b–l), for 1 h at 37 °C. The samples in lane c–l are **1–9**, and $\mathbf{1H_2}$, respectively.

DNA (Form III) in 8% yield. Compounds **8** and **9** were much more efficient at mediating DNA relaxation than **1**; especially, **8** induced the complete degradation of linear DNA (Form III) as indicated by the smearing of the band. The high potency of **8** and **9** can be attributed to their *ortho*-hydroquinone (catechol) structure, which logically improves their ability to cleave DNA by facilitating the generation of oxygen radicals through the formation of *ortho*-hydroquinone–Cu(II)–O_2 complex. Of particular interest is the difference in the potency between **1** and its 3-hydroxy isomer **2**. A change in the placement of the 4-hydroxy group of **1** to the 3-position resulted in a significant decrease in its ability to cleave DNA. Similar differences were noted in comparing the dihydroxy (**4** vs **5**) and monohydroxy (**6** vs **7**) stilbenes, which is consistent with the suggestion that the 4-hydroxy group is essential for effecting DNA cleavage. Since oxygen radical is believed to be the active species responsible for Cu(II)-dependent DNA cleavage, the 4-hydroxy group in combination of O_2 and Cu(II) may serve to facilitate the generation of oxygen radical. However, **3** was found to be quite efficient at mediating DNA relaxation, which suggests that the 3,5-dihydroxybenzene structure, which is distinct from 3-hydroxybenzene, is also essential for potentiating DNA strand scission.

2.2. Cu(II)-binding ability

It has been shown that several xenobiotics that contain a catechol moiety undergo Cu(II)-mediated oxidation to form reactive oxygen species (ROS) that are capable of causing DNA strand breaks. Sotomatsu et al. demonstrated that Cu(II) and Fe(III) had affinity for the hydroquinone moiety of 3,4-dihydroxyphenylalanine (dopa) and, after coordinating with dopa, promoted the peroxidative cleavage of unsaturated phospholipids.[20] Since **1** can coordinate Cu(II), its binding ability has been observed as a change in UV absorption spectra using a Cu(II) titration experiment, whereas no such binding has been observed in the case of Fe(III).[8] Considering the unique specificity of Cu(II), which may induce DNA strand scission of **1**, the ability of **1** to bind to Cu(II) might be advantageous for generating ROS and inducing Cu(II)-dependent DNA scission. Therefore, to elucidate the structural component of **1** that is responsible for its Cu(II)-binding ability, the UV spectra of **1** and its analogues (**2**–**7** and $\mathbf{1H_2}$) in various concentrations of Cu(II) were observed, and their Cu(II)-binding abilities were compared. As shown in Figure 3, the incremental addition of Cu(II) to 20 μM of **1** resulted in a blueshift of the peak from 220 to 210 nm with a concomitant increase in absorbance and a decrease in the absorbance at 308 nm, consistent with the binding of **1** with Cu(II). This spectral change reflects a 1:1 stoichiometry for the complex between **1** and Cu(II), and the binding constant was determined to be $1.75 \times 10^7\ M^{-1}$. Figure 4 shows the effect of the Cu(II) concentration on the absorbance of **1** and its analogues in the range 270–330 nm. A decrease in absorbance, similar to that of **1** at 308 nm, was observed for 3,4- and 4-hydroxy analogues of **4** and **7** at 324 and 304 nm, respectively, indicating that the change is due to its coordination with

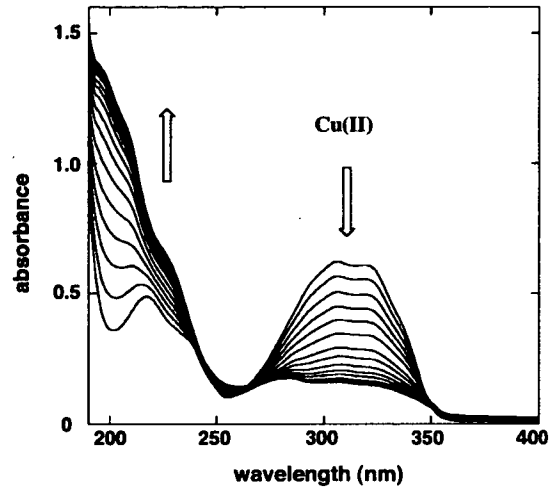

Figure 3. Spectral changes observed upon addition of $CuCl_2$ (0–30 μM) to a sodium cacodylate buffer (pH 7.1)/CH_3CN mixed solution of **1** (20 μM).

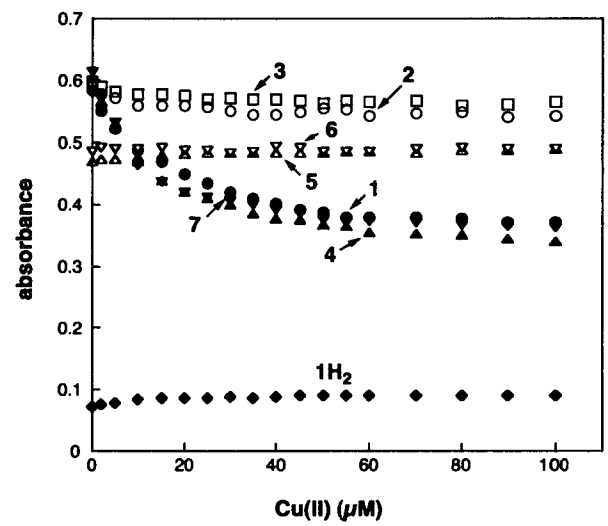

Figure 4. Changes in the absorbance (λ_{max}) of **1** and its analogues (20 μM) upon the addition of $CuCl_2$ (0–100 μM).

Cu(II). In contrast, with an increase in the concentration of Cu(II), there was little or no effect on the absorbance of **2**, **3**, **5**, and **6**, which lacked a 4-hydroxy group on the stilbene moiety, at 306, 300, 298, and 298 nm, respectively, suggesting that ligation of these compounds to Cu(II) did not occur. Further, only a slight effect was observed for dihydroresveratrol $\mathbf{1H_2}$. These results constitute strong evidence that the 4-hydroxy group of **1** is essential for Cu(II) coordination and the ability of the 4-hydroxy group to bind with Cu(II) depends on the structure of stilbene.

2.3. DNA-binding ability

Since **1** is capable of binding to DNA,[19] ROS produced by **1** in combination with Cu(II) might be effective at mediating DNA relaxation. Therefore, to

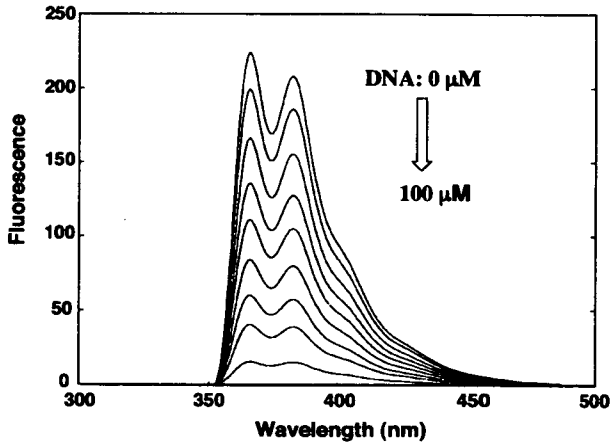

Figure 5. Effect of calf thymus DNA on the fluorescence emission (excitation wavelength 260 nm) of **1**. Trace 1 is the emission spectrum of **1** alone (20 μM); traces 2–9 are emission spectra of **1** in the presence of 2, 5, 10, 15, 20, 30, 50, and 100 μM DNA bp, respectively.

characterize the interaction of **1** with DNA, the ability of **1** and its analogues to bind DNA was estimated by fluorescence titration. The fluorescence emission spectra of **1** in the presence of calf thymus DNA are shown in Figure 5. As indicated, the addition of DNA to **1** causes a decrease in fluorescence emission, and, without any modification of the spectral shape, a decrease in the degree of fluorescence is seen with an increasing concentration of DNA, suggesting that **1** binds to duplex DNA not via groove binding but rather through significant intercalation. In fact, denatured DNA does not appreciably quench the fluorescence of **1** (data not shown). Stern–Volmer plots of the quenching of the fluorescence of **1** and its analogues (**2**–**7** and $\mathbf{1H_2}$) by calf thymus DNA are shown in Figure 6. Native DNA quenches the fluorescence of **1** five times more efficiently than it quenches $\mathbf{1H_2}$,

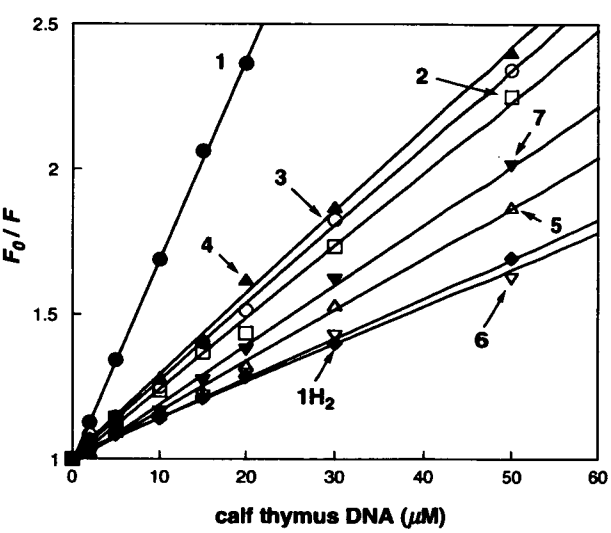

Figure 6. Stern–Volmer plot of quenching of the fluorescence of **1** and its analogues by calf thymus DNA.

indicating that the planarity of the stilbene structure is effective for binding with the duplex DNA structure, probably by taking advantage of its stacking against the base pair. Figure 6 also indicates that phenolic hydroxyl groups attached to the stilbene structure greatly affect the DNA-binding affinity. An increase in the number of hydroxyl groups tends to increase the DNA-binding affinity, which is consistent with the suggestion that the number of phenolic hydroxyl groups is important for its DNA-binding affinity. However, the binding affinity is also determined by the combination of the number and localization of phenolic hydroxyl groups. Thus, the fluorescence of isoresveratrol **2**, in which the 4-hydroxy group of resveratrol **1** is changed to the 3-position, was quenched by DNA with low efficiency ($K_{sv} = 2.40 \times 10^4\ M^{-1}$) compared to **1** ($K_{sv} = 6.80 \times 10^4\ M^{-1}$), and the same results were also observed with dihydroxyl (**4** vs **5**) and monohydroxyl (**7** vs **6**) stilbenes, suggesting that the 4-hydroxy group may be the essential component for binding DNA and plays an important role in specific hydrogen bond interactions with DNA.

2.4. ESR analysis

To confirm the electrostatic interaction of hydroxylated stilbenes with both Cu(II) and DNA, ESR signals of Cu(II) were observed in the presence of **1** or its analogues together with calf thymus DNA. Once the ternary complex of Cu(II)-**1**-DNA, which is due to the efficient binding affinities of **1** with both Cu(II) and DNA, is formed, the complex may result due to its high DNA-cleaving ability. Figure 7 shows that an ESR signal of Cu(II) became multiple upon the addition of DNA, consistent with the fact that Cu(II) complexes DNA. In fact, the decrease in the peak height of Cu(II) in a solution of calf thymus DNA is due to the intercalation of Cu(II) with a large molecule of DNA, which limits the mobility of Cu(II). When **1** was added to the solution of Cu(II)–DNA complex, the peak height of the ESR signal was reduced to one-half of that of the Cu(II)–DNA complex and the resonance was weakened, suggesting that **1** was bound to Cu(II)–DNA complex and thus induced the reduction of Cu(II), which was converted to an ESR-silent species, very likely Cu(I). If the binding of Cu(II) to DNA decreases with the addition of **1**, the signal of Cu(II) should increase to the height of unbound Cu(II). An increase in peak height was also not observed for other resveratrol analogues, suggesting that Cu(II) remains in a complex with DNA even after the addition of **1** and its analogues. Compared to the reduction of Cu(II) to Cu(I) by **1**, an efficient reduction of the peak height of Cu(II)–DNA complex was not observed with the addition of isoresveratrol **2**. It is possible that the insufficient binding affinity of **2** with both DNA and Cu(II) may impair the highly efficient reduction of Cu(II) to Cu(I). Similarly, **7** affected the spectra of Cu(II)–DNA with efficient reducing and broadening, whereas there was no effect on the spectra of Cu(II)–DNA upon the addition of **6**, indicating that the reductive activation of Cu(II) is accelerated by electrostatic interaction of a hydroxyl group at the 4-position.

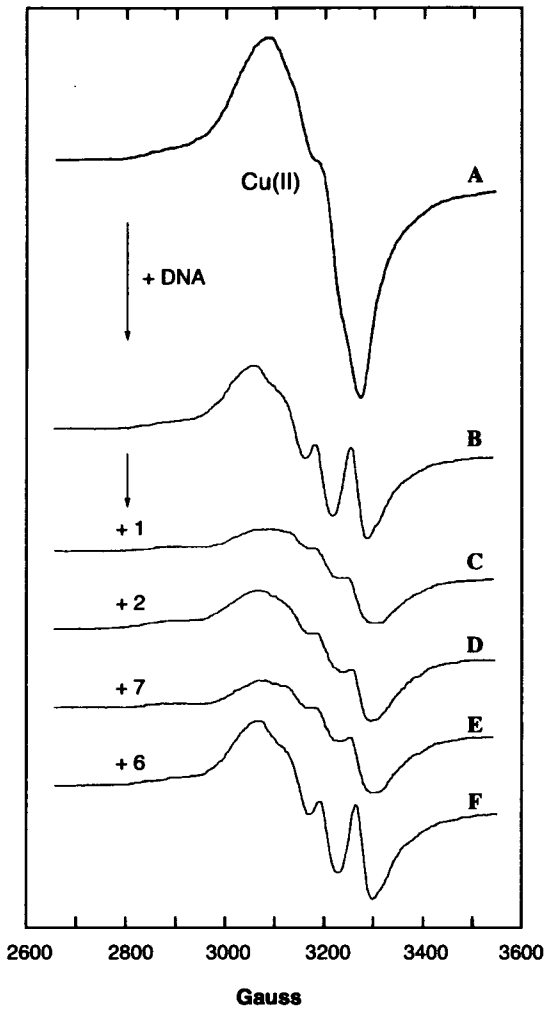

Figure 7. Effect of **1** and its analogues on the ESR spectra of Cu(II) in the presence of calf thymus DNA. Spectra A is 1 mM $CuCl_2$ and spectra B–F show after the addition of 2 mM NP of calf thymus DNA in the absence (B) or presence of 1 mM chemicals (C: **1**; D: **2**; E: **7**; F: **6**). All spectra were recorded after incubation for 30 min at room temperature.

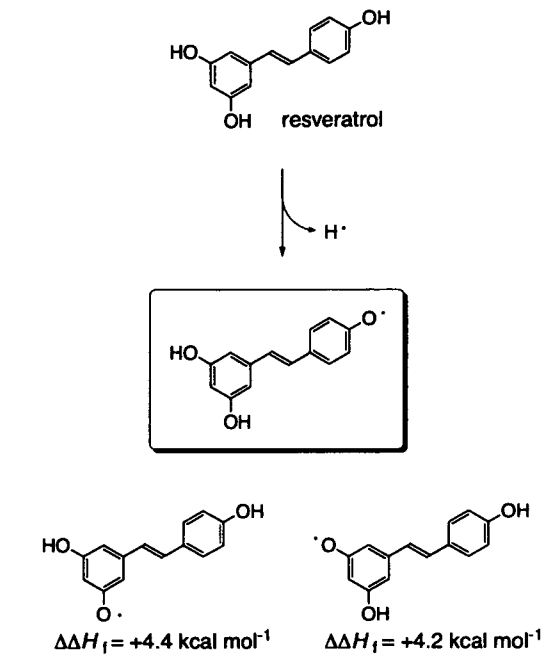

Figure 8. Relative energy values ($\Delta\Delta H_f$) of three types of resveratrol radicals calculated by the DFT calculation, B3LYP/6-31G* basis set.

3. Conclusion

In general, polyphenols, which are responsible for reactive oxygen-associated toxicity, appear to play an important role in the reductive activation of molecular oxygen by its autooxidation, which, in most cases, is coupled with the formation of redox active *ortho-* or *para*-quinones. Catechol is the typical polyphenol that is essential for generating oxygen radical in the presence of Cu(II).[21] It is formed as an activated metabolite of polycyclic aromatic hydrocarbons, which are known to be ubiquitous environmental pollutants. Although **1** is a polyphenol that is known to be an antioxidant and a potential cancer chemopreventive agent, it cleaved DNA strongly without oxidative transformation to the catechol structure in the presence of Cu(II). The DNA cleavage is attributed to the generation of copper-peroxide complex that is formed by electron transfer from **1** to molecular oxygen.[19] The oxidative product of **1** is a dimer[22] and formation of the catechol structure has not been reported. Therefore, the oxidative dimer might be formed by dimerization of resveratrol radical as a result of the reductive activation of molecular oxygen. In the present work, the number and positions of the hydroxyl groups in the stilbene structure were associated with DNA-cleaving activity and the 4-hydroxy group of stilbene played an especially critical role in DNA cleavage. The high binding affinity of a hydroxyl group at the 4-position with both Cu(II) and DNA makes it possible to form a ternary complex and therefore cleave DNA efficiently. When the heats of formation of three types of resveratrol radicals are compared, as shown in Figure 8, the 4-oxyl radical of **1** is the most stable, indicating that the hydroxyl group at the 4-position is much more subjected to oxidation than other hydroxyl groups. In fact, the efficient reduction of Cu(II) to Cu(I) was seen with **1**, which has a hydroxyl group at the 4-position, while there was no effect on Cu(II) reduction in the presence of **2** in which the 4-hydroxy group in **1** is moved to the 3-position. The decrease in the DNA-cleaving ability of $\mathbf{1H_2}$ compared to that of **1** also indicated the importance of the stilbene structure, which might be effective not only for DNA binding for the planarity of the overall structure but also for the stability of the 4-oxyl radical. These results suggest that the ability of **1** to induce oxidative DNA damage in the presence of Cu(II) can be attributed to the structure of 4-hydroxystilbene which is comparable to that of catechol.

Estrogens have been reported to cause cancer through a genotoxic effect. The genotoxicity of estrogens is attributed to the accumulation of potentially carcinogenic metabolites and almost all of these are the catechol form of estrogens. Catechol estrogen metabolites are capable

of causing chromosomal aberrations and gene mutations in cultured cells. The oxidative DNA damage and/or alkylation of DNA that is responsible for the risk of developing cancer are also induced by catechol estrogen metabolites. In fact, the catechol structure, which can cause genotoxicity, is capable of inducing DNA strand scission and the oxidation of DNA bases in the presence of Cu(II). Recently, we reported the genotoxicity of **1**, which induced micronucleus, sister chromatid exchange, and S phase arrest.[23] Among the many types of hydroxylated stilbenes, 4-hydroxystilbene most effectively caused genotoxic effects. Therefore, the finding that the 4-hydroxylstilbene structure is responsible for various biological activities, especially DNA damage leading to genotoxicity, might be important for understanding the toxicity of polyphenols that do not have a catechol structure.

4. Experimental

4.1. Materials

Resveratrol **1** and calf thymus DNA were purchased from Sigma (St. Louis, MO). Supercoiled plasmid pBR322DNA was purchased from Nippon Gene (Tokyo, Japan). Analogues of **1**; 3,5,3′-trihydroxy- (**2**), 3,5-dihydroxy- (**3**), 3,4′-dihydroxy- (**4**), 3,3′-dihydroxy- (**5**), 3-hydroxy- (**6**), 4-hydroxy (**7**), 3,4,3′,5′-tetrahydroxy- (**8**), and 3,4,3′-trihydroxy-*trans*-stilbene (**9**), as shown in Figure 1, were synthesized as previously reported.[24] Saturated form of **1** (**1H$_2$**) was synthesized by hydrogenation of **1** using 10% Pd/C as catalyst. Yield: 98%. ^{1}H NMR(acetone-d_6): δ 2.73 (m, 4H), 6.19 (d, 1H, J = 2.0 Hz), 6.22 (d, 1H, J = 2.0 Hz), 6.74 (d, 2H, J = 8.4 Hz), 7.03 (d, 2H, J = 8.4 Hz). All other chemicals and solvents were of reagent grade or better.

4.2. DNA-cleaving activity

DNA strand breakage was measured in terms of the conversion of supercoiled pBR322 plasmid DNA to the open circular and linear forms. Reactions were carried out in 20 μL (total volume) of 50 mM Na cacodylate buffer (2.5% DMF), pH 7.2, containing 45 μM bp pBR322 DNA, 10 μM $CuCl_2$, and 100 μM of each stilbene derivative. The reaction mixtures were incubated at 37 °C for 1 h and then treated with 5 μL of loading buffer (100 mM TBE buffer, pH 8.3, containing 30% glycerol, 0.1% bromophenol blue) and applied to 1% agarose gel. Horizontal gel electrophoresis was carried out in 50 mM TBE buffer, pH 8.3. The gels were stained with ethidium bromide (1 μg mL^{-1}) for 30 min, destained in water for 30 min, and photographed with UV translumination.

4.3. UV–visible spectra measurements

UV–visible spectra were measured at 37 °C with a Hewlett Packard 8452A Diode Array Spectrophotometer. A solution in a final volume of 1 mL consisted of 20 μM of sample and 0–100 μM $CuCl_2$ in sodium cacodylate buffer (pH 7.1)/acetonitrile mixed solvent (1:1 v/v) was prepared and subjected to spectral analysis. The binding constant between **1** and Cu(II) was obtained according to the method described by Itoh et al.[25]

4.4. Fluorescence measurements

Fluorescence excitation and emission spectra were recorded on a Shimadzu RF-5300PC. A solution in a final volume of 1 mL, which consisted of 20 μM of sample and 0–100 μM calf thymus DNA in 10 mM sodium cacodylate buffer (pH 7.1) and DMF (10% by volume), was used for fluorescence-quenching experiments. The excitation wavelengths used were 255 nm for **1**, **3**, **6**, and **7**, and 260 nm for **2**, **4**, **5**, and **1H$_2$**, and emissions were recorded in the range of 300–500 nm. For all experiments, the sample temperature was maintained at 37 °C. The quenching data were analyzed by the Stern–Volmer equation:[26]

$$F_0/F = 1 + K_{sv}[Q],$$

where [Q] is the molar concentration of the calf thymus DNA, F_0 and F are the fluorescence intensities in the absence and in the presence of the calf thymus DNA [Q], respectively, and K_{sv} is the Stern–Volmer quenching constant.

4.5. ESR analysis

ESR spectra were recorded at room temperature on a JES-FE 2XG spectrometer (JEOL Co. Ltd., Tokyo, Japan). The sample containing 1 mM $CuCl_2$, 2 mM NP of calf thymus DNA, and 1 mM of chemical in 50 mM phosphate buffer (pH 7.2) and acetonitrile (5% by volume) was introduced into a quartz flat cell and incubated at room temperature for 30 min. The ESR spectrum was then recorded. The spectrometer settings were modulation frequency, 100 kHz; modulation amplitude, 10 G; and microwave power, 16 mW.

4.6. Theoretical calculations

Density functional calculations were performed with Gaussian03 (Revision C.02, Gaussian, Inc.) using the unrestricted B3LYP functional for the open shell molecule on an 8-processor QuantumCube™ developed by Parallel Quantum Solutions.

Acknowledgments

This work was supported partly by a grant (MF-16) from the Organization for Pharmaceutical Safety and Research of Japan, a grant from the Ministry of Health, Labour and Welfare, a Grant-in-Aid for Research of Health Sciences focusing on Drug Innovation (KH51058) from the Japan Health Sciences Foundation, and partly by Grants-in-Aid for Scientific Research (B) (No. 17390033) and for Young Scientist (B) (No. 17790044) from the Ministry of Education, Culture, Sports, Science and Technology, Japan.

References and notes

1. Hirano, R.; Sasamoto, W.; Matsumoto, A.; Itakura, H.; Igarashi, O.; Kondo, K. *J. Nutr. Sci. Vitaminol. (Tokyo)* **2001**, *47*, 357.
2. Witztum, J. L.; Steinberg, D. *J. Clin. Invest.* **1991**, *88*, 1785.
3. Steinberg, D. *J. Biol. Chem.* **1997**, *272*, 20963.
4. Hayek, T.; Fuhrman, B.; Vaya, J.; Rosenblat, M.; Belinky, P.; Coleman, R.; Elis, A.; Aviram, M. *Arterioscler. Thromb. Vasc. Biol.* **1997**, *17*, 2744.
5. Jeandet, P.; Bessis, R.; Gautheron, B. *Am. J. Enol. Vitic.* **1991**, *42*, 41.
6. Langcake, P.; Pryce, R. *J. Physiol. Plant Pathol.* **1976**, *9*, 77.
7. Frankel, E. N.; Waterhouse, A. L.; Kinsella, J. E. *Lancet* **1993**, *341*, 1103.
8. Belguendouz, L.; Fremont, L.; Linard, A. *Biochem. Pharmacol.* **1997**, *53*, 1347.
9. Jang, M.; Pezzuto, J. M. *Drugs Exp. Clin. Res.* **1999**, *25*, 65.
10. Olas, B.; Wachowicz, B.; Stochmal, A.; Oleszek, W. *Platelets* **2002**, *13*, 167.
11. Wu, J. M.; Wang, Z. R.; Hsieh, T. C.; Bruder, K. L.; Zou, J. G.; Huang, Y. Z. *Int. J. Mol. Med.* **2001**, *8*, 3.
12. Jang, M.; Cai, L.; Udeani, G. O.; Slowing, K. V.; Thomas, C. F.; Beecher, C. W.; Fong, H. H.; Farnsworth, N. R.; Kinghorn, A. D.; Mehta, R. G.; Moon, R. C.; Pezzuto, J. M. *Science* **1997**, *275*, 218.
13. Jang, M.; Pezzuto, J. M. *Drug Exp. Clin. Res.* **1999**, *25*, 65.
14. Mgbonyebi, O. P.; Russo, J.; Russo, I. H. *Int. J. Oncol.* **1998**, *12*, 865.
15. Uenobe, F.; Nakamura, S.; Miyazawa, M. *Mutat. Res.* **1997**, *373*, 197.
16. Kim, H. J.; Chang, E. J.; Bae, S. J.; Shim, S. M.; Park, H. D.; Rhee, C. H.; Park, J. H.; Choi, S. W. *Arch. Pharm. Res.* **2002**, *25*, 293.
17. Lindenberg, B. A.; Massin, M. J. *J. Physiol. (Paris)* **1957**, *49*, 285.
18. Scannell, R. T.; Barr, J. R.; Murty, V. S.; Reddy, K. S.; Hecht, S. M. *J. Am. Chem. Soc.* **1988**, *110*, 3650.
19. Fukuhara, K.; Miyata, N. *Bioorg. Med. Chem. Lett.* **1998**, *8*, 3187.
20. Sotomatsu, A.; Nakano, M.; Hirai, S. *Arch. Biochem. Biophys.* **1990**, *283*, 334.
21. Seike, K.; Murata, M.; Oikawa, S.; Hiraku, Y.; Hirakawa, K.; Kawanishi, S. *Chem. Res. Toxicol.* **2003**, *16*, 1470.
22. Wang, M.; Jin, Y.; Ho, C.-T. *J. Agric. Food Chem.* **1999**, *47*, 3974.
23. Matsuoka, A.; Takeshita, K.; Furuta, A.; Ozaki, M.; Fukuhara, K.; Miyata, N. *Mutat. Res.* **2002**, *521*, 29.
24. Thakkar, K.; Geahlen, R. L.; Cushman, M. *J. Med. Chem.* **1993**, *36*, 2950.
25. Itoh, S.; Taniguchi, M.; Takada, N.; Nagatomo, S.; Kitagawa, T.; Fukuzumi, S. *J. Am. Chem. Soc.* **2000**, *122*, 12087.
26. Barcelo, F.; Barcelo, I.; Gavilanes, F.; Ferragut, J. A.; Yanovich, S.; Gonzalez-Ros, J. M. *Biochim. Biophys. Acta* **1986**, *884*, 172.

J. Appl. Glycosci., 53, 255–260 (2006)

Regular Paper

Design and Synthesis of α-Glucosidase Inhibitor Having DNA Cleaving Activity

(Received May 15, 2006; Accepted July 10, 2006)

Wataru Hakamata,[1,*] Emiko Yamamoto,[1,2] Makoto Muroi,[3] Masataka Mochizuki,[2] Masaaki Kurihara,[1] Haruhiro Okuda[1] and Kiyoshi Fukuhara[1]

[1]*Division of Organic Chemistry, National Institute of Health Sciences (NIHS) (1–18–1, Kamiyoga, Setagaya-ku, Tokyo 158–8501, Japan)*
[2]*Division of Organic and Bioorganic Chemistry, Kyoritsu University of Pharmacy (1–5–30, Shibakoen, Minato-ku, Tokyo 105–8512, Japan)*
[3]*Antibiotics Laboratory, The Institute of Physical and Chemical Research (RIKEN) (2–1, Hirosawa, Wako 351–0198, Japan)*

Abstract: Apoptosis, or programmed cell death, is a mechanism by which cells undergo death to control cell proliferation or in response to DNA damage. The present study was designed to explore small molecule apoptosis inducers for antitumor agents. The synthesis of 4-sulfonylphenyl α-D-glucopyranoside derivatives 1–6 and 4-(sulfonylamino)phenyl α-D-glucopyranoside derivatives 7–12, endoplasmic reticulum (ER)-targeted small molecules that were designed to induce apoptosis from ER stress by ER glucosidase inhibition and DNA damage is described. Compounds 6 and 12, with a terminal 2-naphthyl group, indicated inhibitions of α-glucosidases from *S. cerevisiae* (IC_{50}=51.7 μM and IC_{50}=74.1 μM) and *B. stearothermophilus* (IC_{50}=60.1 μM and IC_{50}=89.1 μM). Moreover, compound 12 strongly induced the DNA strand breakage condition. When compounds 1–12 were assayed for their ability to inhibit processing by glucosidases at the cellular level, no effects on glycoprotein processing were observed.

Key words: α-glucosidase, inhibitor, DNA cleavage, apoptosis, ER stress

The cell is perturbed by environmental stress conditions. In order to avoid cell death from the stress, cells must sense and respond to stress, including viral infection, genetic mutation, chemical insult, and nutrient depletion.[1] In the ER, stress is a condition that accumulates misfolded or unfolded proteins by disturbing these ER circumstances. Specific response programs are activated to circumvent each type of stress. The ER stress induces a coordinated adaptive program called the unfolded protein response (UPR).[2] The UPR is activated upon disruption of the ER environment by such events as the inhibition of *N*-linked oligosaccharide processing, which results in the accumulation of unfolded or misfolded proteins in the ER.[3] *N*-Linked oligosaccharide processing is carried out by ER glucosidases I and II. Both enzymes are key enzymes in the biosynthesis of *N*-linked oligosaccharides that catalyze the first processing event after the transfer of $Glc_3Man_9GlcNAc_2$ to proteins.[4] The inhibition of ER glucosidases induces the accumulation of unfolded proteins in the ER, and increases ER stress. The UPR caused by ER stress is insulted due to DNA damage, and the cell is led to apoptosis. Apoptosis targets are currently being explored for antitumor agent discovery, such as the tumor-necrosis factor (TNF)-related apoptosis-inducing ligand (TRAIL) receptors, the BCL2 family of anti-apoptotic proteins, and inhibitor of apoptosis (IAP) proteins.[1,5]

We think that the inhibition of ER glucosidases can be used to trigger ER stress, and that the ER stress may trigger the UPR. Further, following interruption of the UPR by DNA damage, the cell is led to apoptosis. We think that compounds that have α-glucosidase inhibitory activity and DNA breakage activity may be developed into an ER-targeted small molecule apoptosis inducer for use as an antitumor agent. We have already elucidated the molecular recognition properties[6–13] and the inhibition[13,14] of α-glycosidases necessary for the molecular design of glycosidase inhibitors using synthetic probes. Based on our knowledge, we designed compounds **1–12** to have α-glucosidase inhibitory activity and DNA breakage activity (Fig. 1). The enzymatic liberation of the aglycon from compounds **1–12** might be followed by the ejection of a R^2SO_2H with the concomitant formation of *p*-benzoquinone or *p*-benzoquinone imine,[15] which would then generate reactive oxygen species (ROS), leading to DNA breakage,[16] shown in Fig. 2. The group of Taylar *et al.* has developed a series of 4-(sulfonylamino)phenyl α-D-glucopyranosides.[15] These compounds have been reported to act as competitive yeast α-glucosidase inhibitors. We suspect that these compounds may also be enhanced in their inhibitory activity by changing the sulfonamide of 4-(sulfonylamino)phenyl α-D-glucopyranoside to sulfonate, since the liberation of *p*-benzoquinone is easier than that of *p*-benzoquinone imine.

In this report, we first describe the design and synthesis series of 4-sulfonylphenyl α-D-glucopyranoside derivatives **1–6** and 4-(sulfonylamino)phenyl α-D-glucopyranoside derivatives **7–12**. These compounds **1–12** were evaluated with regard to their ability to inhibit three kinds of α-glucosidases, and the effects of α-glucosidase triggered

* Corresponding author (Tel. +81–3–3700–1141, Fax. +81–3–3707–6950; E-mail: hakamata@nihs.go.jp).

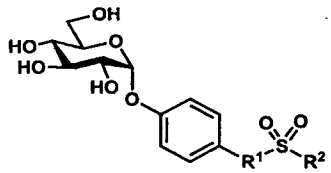

1: R^1=O, R^2=4-NO_2-C_6H_4
2: R^1=O, R^2=4-Cl-C_6H_4
3: R^1=O, R^2=4-CF_3-C_6H_4
4: R^1=O, R^2=4-CH_3-C_6H_4
5: R^1=O, R^2=4-$C(CH_3$-$C_6H_4)_3$
6: R^1=O, R^2=2-naphthyl
7: R^1=NH, R^2=4-NO_2-C_6H_4
8: R^1=NH, R^2=4-Cl-C_6H_4
9: R^1=NH, R^2=4-CF_3-C_6H_4
10: R^1=NH, R^2=4-CH_3-C_6H_4
11: R^1=NH, R^2=4-$C(CH_3)_3$-C_6H_4
12: R^1=NH, R^2=2-naphthyl

Fig. 1. Chemical structure of target compounds **1**–**12**.

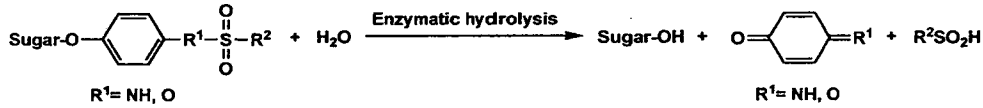

Fig. 2. Schematic diagram of enzymatic liberation of quinone derivatives.

ROS-mediated DNA breakage. Finally, these compounds were also tested in a cell culture system.

MATERIALS AND METHODS

General methods. Optical rotations were measured with a JASCO DIP-370 digital polarimeter at 25°C. The NMR spectra were recorded with a Varian Mercury 400 spectrometer (400 MHz for ^{1}H). Chemical shifts were expressed in ppm downfield relative to Me_4Si. Low resolution mass spectra were obtained with a Waters MicroMass ZQ instrument under positive and negative ion ESI conditions. Column chromatography was performed on silica gel 60 (0.063–0.200 mm, Merck). The progress of all reactions was monitored by thin-layer chromatography on silica gel 60 F_{254} (0.25 mm, Merck).

Method A. To the solution of α-arbutin (**1**, 0.5 g, 1.8 mmol) in 100 mL of dry acetone was added triethylamine (NEt_3, 10 mL) and the sulfonyl chloride derivative (2.8 mmol). After the mixture was stirred for 15 min, the resulting salt was removed by filtration through a cotton filter, and the solvent was concentrated.

Method B. To the solution of α-arbutin (**1**, 1.0 g, 3.7 mmol), in 50 mL of dry acetone was added dry potassium carbonate (K_2CO_3, 1.52 g, 11 mmol) and the sulfonyl chloride derivative (5.5 mmol). After the mixture was stirred overnight, the K_2CO_3 was removed by filtration through Celite, and the solvent was concentrated.

Method C. To the solution of *p*-nitrophenyl α-D-glucopyranoside (**14**, 1.0 g, 3.3 mmol), in pyridine (50 mL) at room temperature was added acetic anhydride (10 mL). The mixture was stirred overnight and poured into water. The product was extracted with AcOEt (3 × 50 mL) and washed with water, 1 M HClaq, satd. $NaHCO_3$aq and brine, and then dried over Na_2SO_4. The product was purified by column chromatography on silica gel (1:1 hexane-AcOEt) to afford a quantitative yield of **15**. A mixture of compound **15** (1.6 g, 3.3 mmol) in ethanol (EtOH, 100 mL) was hydrogenated under H_2 with 20% palladium hydroxide on carbon (150 mg). After the mixture was stirred for 2 h, the palladium charcoal was removed by filtration through Celite and the solvent was concentrated. The product was purified by column chromatography on silica gel (1:1 hexane-AcOEt) to afford 1.5 g (93.9%) of **16**.

Method D. To the solution of compound **16** (0.5 g, 1.2 mmol), in pyridine (20 mL) at room temperature was added sulfonyl chloride derivative (1.36 mmol). The mixture was stirred for 10 min and poured into water. The product was extracted with AcOEt (3 × 50 mL) and washed with water, 1 M HClaq, satd. $NaHCO_3$aq and brine, and then dried over Na_2SO_4, and the solvent was concentrated.

Method E. A mixture of methanol (MeOH) : NEt_3 : H_2O (5:1:1, 60 mL) was added to a stirred solution of the sulfonyl derivative (0.85 mmol). After the mixture was stirred for 6 h at room temperature, the solvent was evaporated.

Synthesis of compounds 1–12.

4-(4-Nitrobenzenesulfonyl)phenyl α-D-glucopyranoside (1). According to method A, compound **1** was prepared from **13** (0.5 g, 1.8 mmol). The product was purified by column chromatography on silica gel (5:1 dichloromethane (CH_2Cl_2)-MeOH) to afford 0.46 g (54.8%) of **2**: $[\alpha]_D$ +14.9° (*c* 0.93, MeOH); ^{1}H NMR (CD_3OD) δ 3.38 (dd, 1H, J_{3-4}=8.8 Hz, J_{4-5}=10.0 Hz, H-4), 3.55 (dd, 1H, J_{1-2}= 3.8 Hz, J_{2-3}=9.8 Hz, H-2), 3.58 (ddd, 1H, J_{4-5}=10.0 Hz, J_{5-6a}=5.2 Hz, J_{5-6b}=2.4 Hz, H-5), 3.67 (dd, 1H, J_{5-6a}=5.0 Hz, J_{6a-6b}=11.8 Hz, H-6a), 3.73 (dd, 1H, J_{5-6b}=2.4 Hz, J_{6a-6b}=12.0 Hz, H-6b), 3.80 (dd, 1H, J_{2-3}=J_{3-4}=9.2 Hz, H-3), 5.42 (d, 1H, *J*=3.6 Hz, H-1), 6.95 (d, 2H, *J*=8.8 Hz, -OC_6H_4O-), 7.12 (d, 2H, *J*=9.2 Hz, -OC_6H_4O-), 8.07 (d, 2H, *J*=9.2 Hz, -$SO_2C_6H_4NO_2$-), 8.44 (d, 2H, *J*=9.2 Hz, -$SO_2C_6H_4NO_2$), MS: 480 $(M+Na)^+$.

4-(4-Chlorobenzenesulfonyl)phenyl α-D-glucopyranoside (2). According to method A, compound **2** was prepared from **13** (0.5 g, 1.8 mmol). The product was purified by column chromatography on silica gel (5:1 CH_2Cl_2-MeOH) to afford 0.59 g (72.5%) of **3**: $[\alpha]_D$ +13.8° (*c* 1.51, MeOH); ^{1}H NMR (CD_3OD) δ 3.40 (dd, 1H, J_{3-4}=9.0 Hz, J_{4-5}=9.8 Hz, H-4), 3.55 (dd, 1H, J_{1-2}=3.6 Hz, J_{2-3}=9.6 Hz, H-2), 3.59 (ddd, 1H, J_{4-5}=10.0 Hz, J_{5-6a}=5.4 Hz, J_{5-6b} =2.2 Hz, H-5), 3.67 (dd, 1H, J_{5-6a}=5.4 Hz, J_{6a-6b}=12 Hz, H-6a), 3.73 (dd, 1H, J_{5-6b}=2.4 Hz, J_{6a-6b}=12.0 Hz, H-6b), 3.81 (dd, 1H, J_{2-3}=9.6 Hz, J_{3-4}=9.2 Hz, H-3), 5.43 (d, 1H, *J*=3.6 Hz, H-1), 6.92 (d, 2H, *J*=9.6 Hz, -OC_6H_4O-), 7.12 (d, 2H, *J*=9.2 Hz, -OC_6H_4O-), 7.62 (d, 2H, *J*=8.8 Hz, -$SO_2C_6H_4Cl$), 7.78 (d, 2H, *J*=8.8 Hz, -$SO_2C_6H_4Cl$), MS: 469 $(M+Na)^+$.

4-(4-Trifluorobenzenesulfonyl)phenyl α-D-glucopyranoside (3). According to method A, compound **3** was prepared from **13** (0.5 g, 1.8 mmol). The product was purified by column chromatography on silica gel (5:1 CH_2Cl_2-MeOH) to afford 0.59 g (88.4%) of **3**: $[\alpha]_D$ +11.7° (*c* 1.25, MeOH); ^{1}H NMR (CD_3OD) δ 3.40 (dd, 1H, J_{3-4}=9.0 Hz, J_{4-5}=9.8 Hz, H-4), 3.55 (dd, 1H, J_{1-2}=3.6 Hz, J_{2-3}= 10.0 Hz, H-2), 3.58 (m, 1H, H-5), 3.66 (dd, 1H, J_{5-6a}=5.0

Hz, J_{6a-6b}=11.8 Hz, H-6a), 3.73 (dd, 1H, J_{5-6b}=2.4 Hz, J_{6a-6b}=12.0 Hz, H-6b), 3.81 (dd, 1H, J_{2-3}=J_{3-4}=9.4 Hz, H-3), 5.43 (d, 1H, J=3.6 Hz, H-1), 6.93 (d, 2H, J=9.2 Hz, -OC_6H_4O-), 7.12 (d, 2H, J=9.2 Hz, -OC_6H_4O-), 7.94 (d, 2H, J=8.0 Hz, -$O_2C_6H_4O$-), 8.02 (d, 2H, J=8.4 Hz, -$SO_2C_6H_4CF_3$), MS: 503 $(M+Na)^+$.

4-(4-Methylbenzenesulfonyl)phenyl α-D-glucopyranoside (4). According to method B, compound **4** was prepared from **13** (1.1 g, 5.5 mmol). The product was purified by column chromatography on silica gel (5:1 CH_2Cl_2-MeOH) to afford 1.03 g (63.4%) of **4**: $[\alpha]_D$ +18.4° (*c* 0.97, MeOH); ^1H NMR (CD_3OD) δ 2.44 (s, 3H, -CH_3), 3.39 (dd, 1H, J_{3-4}=8.8 Hz, J_{4-5}=10.0 Hz, H-4), 3.54 (dd, 1H, J_{1-2}=3.8 Hz, J_{2-3}=9.8 Hz, H-2), 3.58 (ddd, 1H, J_{4-5}= 10.0 Hz, J_{5-6a}=5.2 Hz, J_{5-6b}=2.4 Hz, H-5), 3.66 (dd, 1H, J_{5-6a}=5.2 Hz, J_{6a-6b}=12.0 Hz, H-6a), 3.73 (dd, 1H, J_{5-6b}= 2.6 Hz, J_{6a-6b}=11.8 Hz, H-6b), 3.80 (dd, 1H, J_{2-3}=9.8, J_{3-4} =9.0 Hz, H-3), 5.41 (d, 1H, J=3.6 Hz, H-1), 6.88 (d, 2H, J=9.6 Hz, -OC_6H_4O-), 7.09 (d, 2H, J=9.2 Hz, -OC_6H_4O-), 7.40 (d, 2H, J=8.0 Hz, -$SO_2C_6H_4CH_3$), 7.66 (d, 2H, J=8.4 Hz, -$SO_2C_6H_4CH_3$), MS: 449 $(M+Na)^+$.

4-(4-*tert*-Butylbenzenesulfonyl)phenyl α-D-glucopyranoside (5). According to method B, compound **3** was prepared from **13** (0.5 g, 1.8 mmol). The product was purified by column chromatography on silica gel (5:1 CH_2Cl_2-MeOH) to afford 0.39 g (43.9%) of **5**: $[\alpha]_D$ +13.6° (*c* 1.40, MeOH); ^1H NMR (CD_3OD) δ 1.36 (s, 9H, -$C(CH_3)_3$), 3.39 (dd, 1H, J_{3-4}=8.8 Hz, J_{4-5}=10.0 Hz, H-4), 3.54 (dd, 1H, J_{1-2}=3.6 Hz, J_{2-3}=9.6 Hz, H-2), 3.59 (ddd, 1H, J_{4-5}=10.0 Hz, J_{5-6a}=5.0 Hz, J_{5-6b}=2.5 Hz, H-5), 3.66 (dd, 1H, J_{5-6a}=5.0 Hz, J_{6a-6b}=11.8 Hz, H-6a), 3.73 (dd, 1H, J_{5-6b}=2.4 Hz, J_{6a-6b}=12.0 Hz, H-6b), 3.80 (dd, 1H, J_{2-3} =J_{3-4}=9.4 Hz, H-3), 5.41 (d, 1H, J=3.6 Hz, H-1), 6.89 (d, 2H, J=9.2 Hz, -OC_6H_4O-), 7.10 (d, 2H, J=9.2 Hz, -OC_6H_4O-), 7.64 (d, 2H, J=8.8 Hz, -$SO_2C_6H_4C(CH_3)_3$), 7.72 (d, 2H, J=8.8 Hz, -$SO_2C_6H_4C(CH_3)_3$), MS: 491 $(M+Na)^+$.

4-(2-Naphthalenesulfonyl)phenyl α-D-glucopyranoside (6). According to method B, compound **6** was prepared from **13** (0.5 g, 1.8 mmol). The product was purified by column chromatography on silica gel (5:1 CH_2Cl_2-MeOH) to afford 0.63 g (74.6%) of **6**: $[\alpha]_D$ +12.3° (*c* 1.32, MeOH); ^1H NMR (CD_3OD) δ 3.38 (dd, 1H, J_{3-4}=8.8 Hz, J_{4-5}=10.0 Hz, H-4), 3.52 (dd, 1H, J_{1-2}=3.6 Hz, J_{2-3}=9.6 Hz, H-2), 3.55 (ddd, 1H, J_{4-5}=10.0 Hz, J_{5-6a}=4.8 Hz, J_{5-6b} =2.8 Hz, H-5), 3.64 (dd, 1H, J_{5-6a}=4.8 Hz, J_{6a-6b}=12.0 Hz, H-6a), 3.68 (dd, 1H, J_{5-6b}=2.8 Hz, J_{6a-6b}=12.0 Hz, H-6b), 3.78 (dd, 1H, J_{2-3}=J_{3-4}=9.0 Hz, H-3), 5.38 (d, 1H, J=3.6 Hz, H-1), 6.89, 7.05 (d, 2H × 2, J=9.6 Hz, -OC_6H_4O-), 7.64–7.83, 8.00–8.11, 8.35 (m, 7H, -$SO_2C_{10}H_7$), MS: 485 $(M+Na)^+$.

4-(4-Nitrophenylsulfonylamino)phenyl 2,3,4,6-tetra-*O*-acetyl-α-D-glucopyranoside (17). According to methods C and D, compound **17** was prepared from **16** (0.5 g, 1.1 mmol). The product was purified by column chromatography on silica gel (1:1 hexane-AcOEt) to afford 0.67 g (94.6%) of **17**.

4-(4-Chlorophenylsulfonylamino)phenyl 2,3,4,6-tetra-*O*-acetyl-α-D-glucopyranoside (18). According to methods C and D, compound **18** was prepared from **16** (0.4 g, 1.0 mmol). The product was purified by column chromatography on silica gel (1:1 hexane-AcOEt) to afford 0.54 g (93.1%) of **17**.

4-(4-Trifluoromethylphenylsulfonylamino)phenyl 2,3,4,6-tetra-*O*-acetyl-α-D-glucopyranoside (19). According to methods C and D, compound **19** was prepared from **16** (0.4 g, 1.0 mmol). The product was purified by column chromatography on silica gel (1:1 hexane-AcOEt) to afford 0.65 g (99.9%) of **19**.

4-(4-Methlphenylsulfonylamino)phenyl 2,3,4,6-tetra-*O*-acetyl-α-D-glucopyranoside (20). According to methods C and D, compound **20** was prepared from **16** (0.5 g, 1.1 mmol). The product was purified by column chromatography on silica gel (1:1 hexane-AcOEt) to afford 0.64 g (93.1%) of **20**.

4-(4-tert-Butylphenylsulfonylamino)phenyl 2,3,4,6-tetra-*O*-acetyl-α-D-glucopyranoside (21). According to methods C and D, compound **20** was prepared from **16** (0.4 g, 1.0 mmol). The product was purified by column chromatography on silica gel (1:1 hexane-AcOEt) to afford 0.55 g (88.5%) of **21**.

4-(2-Naphthalenephenylsulfonylamino)phenyl 2,3,4,6-tetra-*O*-acetyl-α-D-glucopyranoside (22). According to methods C and D, compound **22** was prepared from **16** (0.4 g, 1.0 mmol). The product was purified by column chromatography on silica gel (1:1 hexane-AcOEt) to afford 0.53 g (92.5%) of **22**.

4-(4-Nitrophenylsulfonylamino)phenyl α-D-glucopyranoside (7). According to method E, compound **7** was prepared from **17** (0.7 g, 1.1 mmol). The product was purified by column chromatography on silica gel (5:1 CH_2Cl_2-MeOH) to afford 0.41 g (83.3%) of **7**: $[\alpha]_D$ +12.1° (*c* 1.23, MeOH); ^1H NMR (CD_3OD) δ 3.38 (dd, 1H, J_{3-4}=8.8 Hz, J_{4-5}=10.0 Hz, H-4), 3.53 (dd, 1H, J_{1-2}=3.6 Hz, J_{2-3}= 9.6 Hz, H-2), 3.59 (ddd, 1H, J_{4-5}=10.0 Hz, J_{5-6a}=5.0 Hz, J_{5-6b}=2.4 Hz, H-5), 3.65 (dd, 1H, J_{5-6a}=5.0 Hz, J_{6a-6b}=11.8 Hz, H-6a), 3.72 (dd, 1H, J_{5-6b}=2.4 Hz, J_{6a-6b}=12.0 Hz, H-6b), 3.80 (dd, 1H, J_{2-3}=J_{3-4}=9.2 Hz, H-3), 5.38 (d, 1H, J= 3.6 Hz, H-1), 7.0 (d, 2H, J=8.8 Hz, -OC_6H_4NH-), 7.05 (d, 2H, J=9.2 Hz, -OC_6H_4NH-), 7.91 (d, 2H, J=8.8 Hz, -$SO_2C_6H_4NO_2$), 8.31 (d, 2H, J=8.8 Hz, -$SO_2C_6H_4NO_2$), MS: 455 $(M-H)^-$.

4-(4-Chlorophenylsulfonylamino)phenyl α-D-glucopyranoside (8). According to method E, compound **8** was prepared from **18** (0.54 g, 0.9 mmol). The product was purified by column chromatography on silica gel (5:1 CH_2Cl_2-MeOH) to afford 0.38 g (95.2%) of **8**: $[\alpha]_D$ +13.4° (*c* 1.42, MeOH); ^1H NMR (CD_3OD) δ 3.39 (dd, 1H, J_{3-4} =9.2Hz, J_{4-5}=10.0 Hz, H-4), 3.53 (dd, 1H, J_{1-2}=3.8 Hz, J_{2-3}=9.8 Hz, H-2), 3.60 (ddd, 1H, J_{4-5}=10.0 Hz, J_{5-6a}=4.8 Hz, J_{5-6b}=2.6 Hz, H-5), 3.66 (dd, 1H, J_{5-6a}=4.8 Hz, J_{6a-6b} =11.9 Hz, H-6a), 3.72 (dd, 1H, J_{5-6b}=2.6 Hz, J_{6a-6b}=11.9 Hz, H-6b), 3.80 (dd, 1H, J_{2-3}=J_{3-4}=9.2 Hz, H-3), 5.38 (d, 1H, J=4.0 Hz, H-1), 6.98 (d, 2H, J=9.2 Hz, -OC_6H_4NH-), 7.05 (d, 2H, J=9.6 Hz, -OC_6H_4NH-), 7.48 (d, 2H, J=8.8 Hz, -$SO_2C_6H_4Cl$), 7.65 (d, 2H, J=8.8 Hz, -$SO_2C_6H_4Cl$), MS: 444 $(M-H)^-$.

4-(4-Trifluoromethylphenylsulfonylamino)phenyl α-D-glucopyranoside (9). According to method E, compound **9** was prepared from **19** (0.7 g, 1.0 mmol). The product was purified by column chromatography on silica gel (5:1 CH_2Cl_2-MeOH) to afford 0.44 g (90.9%) of **7**: $[\alpha]_D$ +13.4°

(c 1.10, MeOH); ^{1}H NMR (CD_3OD) δ 3.38 (dd, 1H, J_{3-4} =J_{4-5}=9.4 Hz, H-4), 3.53 (dd, 1H, J_{1-2}=3.6 Hz, J_{2-3}=10.0 Hz, H-2), 3.60 (ddd, 1H, J_{4-5}=9.4 Hz, J_{5-6a}=5.0 Hz, J_{5-6b} =2.4 Hz, H-5), 3.66 (dd, 1H, J_{5-6a}=5.0 Hz, J_{6a-6b}=11.8 Hz, H-6a), 3.72 (dd, 1H, J_{5-6b}=2.4 Hz, J_{6a-6b}=12.0 Hz, H-6b), 3.80 (dd, 1H, J_{2-3}=J_{3-4}=9.4 Hz, H-3), 5.39 (d, 1H, J=3.6 Hz, H-1), 6.99 (d, 2H, J=9.2 Hz, -OC_6H_4NH-), 7.05 (d, 2 H, J=9.2 Hz, -OC_6H_4NH-), 7.79 (d, 2H, J=8.4 Hz, -$SO_2C_6H_4CF_3$), 7.87 (d, 2H, J=8.4 Hz, -$SO_2C_6H_4CF_3$), MS: 478 $(M-H)^-$.

4-(4-Methylphenylsulfonylamino)phenyl α-D-glucopyranoside (10). According to method E, compound **10** was prepared from **20** (0.64 g, 1.1 mmol). The product was purified by column chromatography on silica gel (5:1 CH_2Cl_2-MeOH) to afford a quantitative yield (0.50 g) of **10**: $[\alpha]_D$ +13.0° (c 1.98, MeOH); ^{1}H NMR (CD_3OD) δ 2.37 (s, 3H, -CH_3), 3.39 (dd, 1H, J_{3-4}=9.0 Hz, J_{4-5}=9.8 Hz, H-4), 3.53 (dd, 1H, J_{1-2}=3.6 Hz, J_{2-3}=9.6 Hz, H-2), 3.60 (ddd, 1H, J_{4-5}=9.8 Hz, J_{5-6a}=5.2 Hz, J_{5-6b}=2.4 Hz, H-5), 3.66 (dd, 1H, J_{5-6a}=5.2 Hz, J_{6a-6b}=12.0 Hz, H-6a), 3.72 (dd, 1H, J_{5-6b}=2.4 Hz, J_{6a-6b}=12.0 Hz, H-6b), 3.80 (dd, 1H, J_{2-3}=J_{3-4}=9.2 Hz, H-3), 5.37 (d, 1H, J=3.6 Hz, H-1), 6.97 (d, 2H, J=9.6 Hz, -OC_6H_4NH-), 7.02 (d, 2H, J=9.2 Hz, -OC_6H_4NH-), 7.26 (d, 2H, J=8.4 Hz, -$SO_2C_6H_4CH_3$), 7.57 (d, 2H, J=8.4 Hz, -$SO_2C_6H_4CH_3$), MS: 424 $(M-H)^-$.

4-(4-*tert*-Butylphenylsulfonylamino)phenyl α-D-glucopyranoside (11). According to method E, compound **11** was prepared from **21** (0.55 g, 0.9 mmol). The product was purified by column chromatography on silica gel (5:1 CH_2Cl_2-MeOH) to afford 0.40 g (99.7%) of **7**: $[\alpha]_D$ +11.8° (c 1.47, MeOH); ^{1}H NMR (CD_3OD) δ 1.31 (s, 9H, -C $(CH_3)_3$), 3.39 (dd, 1H, J_{3-4}=9.0 Hz, J_{4-5}=9.8 Hz, H-4), 3.53 (dd, 1H, J_{1-2}=3.6 Hz, J_{2-3}=10.0 Hz, H-2), 3.60 (ddd, 1H, J_{4-5}=9.8 Hz, J_{5-6a}=4.8 Hz, J_{5-6b}=2.4 Hz, H-5), 3.66 (dd, 1H, J_{5-6a}=4.8 Hz, J_{6a-6b}=12.0 Hz, H-6a), 3.72 (dd, 1H, J_{5-6b}=2.4 Hz, J_{6a-6b}=12.0 Hz, H-6b), 3.80 (dd, 1H, J_{2-3}=J_{3-4} =9.4 Hz, H-3), 5.37 (d, 1H, J=3.6 Hz, H-1), 6.99 (d, 2H, J=9.2 Hz, -OC_6H_4NH-), 7.03 (d, 2H, J=9.6 Hz, -OC_6H_4NH-), 7.50 (d, 2H, J=8.4 Hz, -$SO_2C_6H_4C(CH_3)_3$), 7.62 (d, 2H, J =8.8 Hz, -$SO_2C_6H_4C$ $(CH_3)_3$), MS: 466 $(M-H)^-$.

4-(2-Naphthalenephenylsulfonylamino)phenyl α-D-glucopyranoside (12). According to method E, compound **12** was prepared from **22** (0.53 g, 0.9 mmol). The product was recrystallized from hot EtOH to afford a quantitative yield 0.40 g of **12**: $[\alpha]_D$ +12.4° (c 1.24, MeOH); ^{1}H NMR (CD_3OD) δ 3.37 (dd, 1H, J_{3-4}=8.8 Hz, J_{4-5}=9.6 Hz, H-4), 3.50 (dd, 1H, J_{1-2}=3.6 Hz, J_{2-3}=10.0 Hz, H-2), 3.56 (ddd, 1H, J_{4-5}=9.6 Hz, J_{5-6a}=4.6 Hz, J_{5-6b}=2.4 Hz, H-5), 3.63 (dd, 1H, J_{5-6a}=4.6 Hz, J_{6a-6b}=11.8 Hz, H-6a), 3.67 (dd, 1H, J_{5-6b}=2.4 Hz, J_{6a-6b}=11.8 Hz, H-6b), 3.77 (dd, 1H, J_{2-3}=J_{3-4}=9.2 Hz, H-3), 5.33 (d, 1H, J=3.6 Hz, H-1), 7.00 (s, 4H, -OC_6H_4NH-), 7.56–7.72, 7.91–7.96, 8.23 (m, 7H, -$SO_2C_{10}H_7$), MS: 460 $(M-H)^-$.

Biological assays. The α-glucosidase inhibition assays were performed using p-nitrophenyl α-D-glucopyranoside (Aldrich) as a substrate and were assayed using previously reported methods.[13] The DNA breakage activity was investigated using previously reported methods.[16-18] Inhibition assays at the cellular level were performed by previously reported methods.[11]

RESULTS AND DISCUSSION

Synthesis of sulfonate and sulfonamide derivatives.

The synthesis of the sulfonate derivatives **1–6** that were used in the present study is presented in Fig. 3. α-Arbutin **13** was used as a starting material for the synthesis of compounds **1–6**. Compound **13** was sulfonated with 4-nitrobenzenesulfonyl chloride, 4-chlorobenzenesulfonyl chloride, 4-trifluoromethylbenzenesulfonyl chloride, 4-methylbenzenesulfonyl chloride, 4-*t*-butylbenzenesulfonyl chloride, and 2-naphthalenesulfonyl chloride in acetone to give compounds **1–6**, respectively.

The synthesis of the sulfonamide derivatives **7–12** that were used in the present study is presented in Fig. 4. p-Nitrophenyl α-D-glucopyranoside **14** was used as a starting material for the synthesis of compounds **7–12**. Compound **14** was acetylated with acetic anhydride in pyridine to give per-acetylated glucopyranoside **15**. Compound **15** was hydrogenated under H_2 with 20% palladium hydroxide on carbon to give the free-base **16**. Compound **16** was sulfonated with 4-nitrobenzenesulfonyl chloride, 4-chloro-

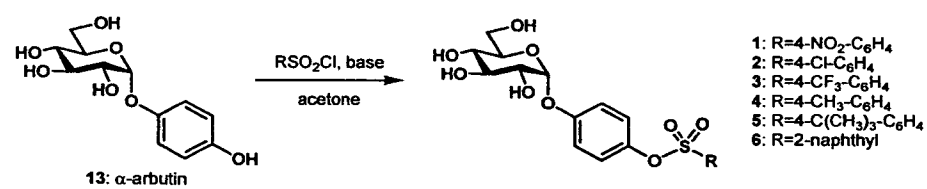

Fig. 3. Synthesis of compounds **1–6**.

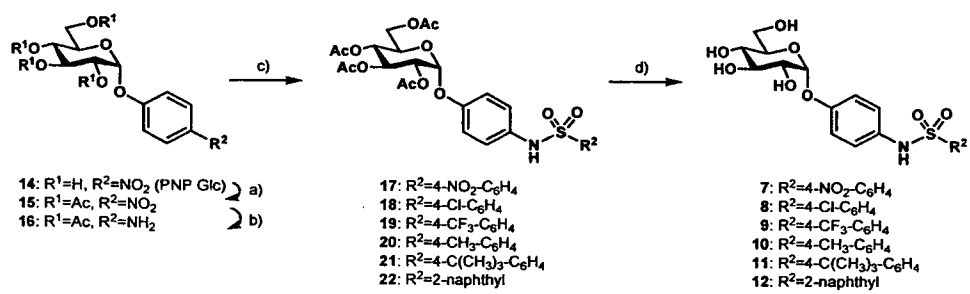

a) Ac_2O, C_5H_5N, b) Pd $(OH)_2$ / C, EtOH, c) R^2SO_2Cl, C_5H_5N, d) NEt_3, H_2O, MeOH

Fig. 4. Synthesis of compounds **7–12**.

benzenesulfonyl chloride, 4-trifluoromethylbenzenesulfonyl chloride, 4-methylbenzenesulfonyl chloride, 4-*t*-butylbenzenesulfonyl chloride, and 2-naphthalenesulfonyl chloride in pyridine to give **17–22** in good yields, respectively. Treatment of the resulting sulfonamides **17–22** with base gave compounds **7–12** in good yields, respectively. To the best of our knowledge, there have been no previous reports on the synthesis of compounds **1–6**, **8–9** or **11**. Data for NMR and MS spectra and optical rotation of all compounds **1–12** have not been reported.

Inhibition of α-glucosidases.

Inhibition studies on compounds **1–12** towards *Saccharomyces cerevisiae, Bacillus stearothermophilus* and rice α-glucosidases, and the results are listed in Table 1. Compounds **6** and **12**, with a terminal 2-naphthyl group, indicated inhibitions of α-glucosidases from *S. cerevisiae* (IC_{50}=51.7 μM and IC_{50}=74.1 μM) and *B. stearothermophilus* (IC_{50}=60.1 μM and IC_{50}=89.1 μM). Compounds **1–5** and **7–11** showed no significant inhibitory properties for *S. cerevisiae* or *B. stearothermophilus* α-glucosidases. No compounds inhibited rice α-glucosidase. Additionally, all α-glucosidases hydrolyzed compounds **1–12**. These results indicated that compounds **1–12** have properties of both substrate and inhibitor against *S. cerevisiae* α-glucosidase. Compounds **1–5** were substrate for *B. stearothermophilus* enzyme. However, compounds **6–12** were substrate and inhibitor for *B. stearothermophilus* enzyme. All compounds were substrate for rice enzyme. From these results if *p*-benzoquinone or *p*-benzoquinone imine are released during the liberation of the aglycon of compounds **1–12**, the huge differences in enzyme inhibitory activity among three kinds of enzymes will not result. This speculation is in conflict with those expected from the theory shown in Fig. 2. Therefore, the enzymatic hydrolysis reaction of compound **4** in the presence of *S. cerevisiae* α-glucosidase was analyzed using the LC/MS system as a model case. It was found that the major product of the hydrolysis reaction was aphenol compound corresponding to the aglycon moiety of compound **4** (data not shown). α-Glucosidase inhibition of compounds **1–12** was considered to be due to the enzymatic formation of phenol derivatives from compounds **1–12**, illustrated in Fig. 5, and/or compounds **1–12** themselves.

DNA Cleavage activities.

Fukuhara *et al.* have reported that a phenol compound, resveratrol, induced Cu(II)-dependent DNA-strand scission under neutral conditions.[17] This DNA cleavage process occurs in the presence of Cu(II) and O_2. The ability of compounds **1–12** to induce DNA cleaving activity was examined using pBR322, a supercoiled, covalently closed circular DNA (Form I), and analyzed by agarose gel electrophoresis (Table 2). α-Glucosidase-triggered radical-mediated DNA breakage was very effectively observed for sulfonamide derivatives **7–12**. Consistent with the fact that Cu(II) and enzyme are required for potent DNA cleaving activity of compounds **7–12**, these compounds induced DNA cleavage only when the reaction was carried out in the presence of Cu(II) and enzyme; in the absence of Cu(II) and enzyme, no DNA cleavage was observed. On the other hand, sulfonate derivatives **1–6** caused only slight damage under the same conditions. The decrease in the DNA cleaving ability of compounds **1–6** compared to that of compounds **7–12** also indicated the importance of the sulfonamide structure, which might be

Table 1. Inhibitory activities of compounds **1–12** against α-glucosidases.

Compound	IC_{50} (μM)		
	S. cerevisaise	*B. stearothermophilus*	Rice
1	499	>500	>500
2	437	>500	>500
3	407	>500	>500
4	499	>500	>500
5	391	>500	>500
6	51.7	60.1	>500
7	239	218	>500
8	200	254	>500
9	146	244	>500
10	231	325	>500
11	136	237	>500
12	74.1	89.1	>500

The *S. cerevisiae* and *B. stearothermophilus* α-glucosidase inhibition assays were performed by using 1 mM PNP Glc as substrate. The assay conditions were potassium phosphate buffer (pH 7.0) at 37°C, 20 min. The rice α-glucosidase inhibition assay was performed by using 1 mM PNP Glc as substrate. The assay conditions were sodium acetate buffer (pH 4.0) at 37°C, 60 min. All α-glucosidases hydrolyzed compounds **1–12**.

Table 2. Enzyme-triggered DNA-cleaving activities of compounds **1–12**.

Compound		Residual ratio of Form I plasmid (%)				
	$CuCl_2$	+	+	−	−	+
	NADH	+	−	+	−	+
	Enzyme	+	+	+	+	−
1		86	100	100	100	100
2		87	100	100	100	100
3		91	72	100	100	100
4		93	100	100	100	100
5		85	100	100	100	100
6		76	64	100	100	100
7		<1	<1	100	100	100
8		<1	<1	100	100	100
9		<1	23	100	100	100
10		<1	17	100	100	100
11		<1	6	100	100	100
12		<1	22	100	100	100

Analysis of DNA strand breaks generated in pBR322DNA with compounds **1–12**. Assays were performed by using 1 mM of compound, 100 μM $CuCl_2$, 500 μM NADH, and *S. cerevisiae* α-glucosidase. The assay conditions were sodium phosphate buffer (pH 7.0) containing pBR322DNA at 37 °C, for 20 h.

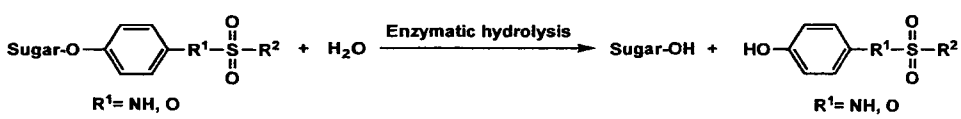

Fig. 5. Schematic diagram of enzymatic liberation of phenol derivatives.

effective not only for DNA binding for the conformation of the overall structure but also for the stability of the phenoxy radical. No effect of DNA cleaving activity of compounds **1**–**12** was observed in spite of the presence of NADH. It would appear that the enzymatic liberation of quinone derivative shown in Fig. 2 does not occur, since quinone derivatives showed DNA cleaving activity in the presence of NADH.[15] These findings can be explained by the fact that enzymatic liberation of the aglycon from compounds **1**–**12** was followed by the ejection of phenol derivatives, shown in Fig. 5.

Cellular level assays.

Compounds **1**–**12** were assayed with regard to their ability to inhibit ER glucosidase at the cellular level. Vesicular stomatitis virus glycoprotein (VSV G) was prepared from VSV-infected and probe-treated baby hamster kidney (BHK) cells. Analyses of the *N*-glycan structure of obtained VSV G using endo H, which is known to have hydrolytic activity against high-mannose type *N*-glycan, failed to confirm that these compounds inhibited ER glucosidases (data not shown).

We have shown that dual functional small molecules having both the α-glucosidase inhibitory activity and DNA breakage activity at the enzyme level can be designed, using our mechanism-based approach. We plan in the near future to study the structure-activity relationship and to extend the same strategies to more complicated cellular systems. We think that ER-targeted small molecule apoptosis inducers are necessary for the development of new and potent antitumor agents.

This research was partly supported by the Ministry of Education, Science, Sports and Culture Grant-in-Aid for Young Scientists (B) (No. 17790097) and Health and Labour Sciences Research Grants for Research on HIV/AIDS to W.H. from the Ministry of Health, Labour and Welfare, Japan. We thank Ezaki Glico Co., Ltd., for the gift of α-arbutin.

REFERENCES

1) U. Fischer and K. Schulze-Osthoff: Apoptosis-based therapies and drug targets. *Cell Death Differ.*, **12**, 942–961 (2005).
2) Y. Ma and L.M. Hendershot: The unfolding tale of the unfolded protein response. *Cell*, **107**, 827–830 (2001).
3) M. Schroder and R.J. Kaufman: ER stress and the unfolded protein response. *Mutat. Res.*, **569**, 29–63 (2005).
4) C.R. Bertozzi and L.L. Kiessling: Chemical glycobiology. *Science*, **291**, 2357–2364 (2001).
5) S.W. Fesik: Promoting apoptosis as a strategy for cancer drug discovery. *Nat. Rev. Cancer*, **5**, 876–885 (2005).
6) T. Nishio, Y. Miyake, H. Tsujii, W. Hakamata, K. Kadokura and T. Oku: Hydrolytic activity of α-mannosidase against deoxy derivatives of *p*-nitrophenyl α-D-mannopyranoside. *Biosci. Biotech. Biochem.*, **60**, 2038–2042 (1996).
7) W. Hakamata, T. Nishio and T. Oku: Synthesis of *p*-nitrophenyl 3- and 6-deoxy-α-D-glucopyranosides and their specificity to rice α-glucosidase. *J. Appl. Glycosci.*, **46**, 459–463 (1999).
8) W. Hakamata, T. Nishio and T. Oku: Hydrolytic activity of α-galactosidase against deoxy derivatives of *p*-nitrophenyl α-D-galactopyranoside. *Carbohydr. Res.*, **324**, 107–115 (2000).
9) W. Hakamata, T. Nishio, R. Sato, T. Mochizuki, K. Tsuchiya, M. Yasuda and T. Oku: Synthesis of monomethyl derivatives of *p*-nitrophenyl α-D-gluco, galacto, and mannopyranosides and their hydrolytic properties against α-glycosidase. *J. Carbohydr. Chem.*, **19**, 359–377 (2000).
10) T. Nishio, W. Hakamata, A. Kimura, S. Chiba, A. Takatsuki, R. Kawachi and T. Oku: Glycon specificity profiling of α-glucosidases using monodeoxy and mono-*O*-methyl derivatives of *p*-nitrophenyl α-D-glucopyranoside. *Carbohydr. Res.*, **337**, 629–634 (2002).
11) W. Hakamata, M. Muroi, T. Nishio, T. Oku and A. Takatsuki: Recognition properties of processing α-glucosidase I and α-glucosidase II. *J. Carbohydr. Chem.*, **23**, 27–39 (2004).
12) T. Nishio, W. Hakamata, M. Ogawa, K. Nakajima, Y. Matsuishi, R. Kawachi and T. Oku: Investigations of useful α-glycosidase for the enzymatic synthesis of rare sugar oligosaccharides. *J. Appl. Glycosci.*, **52**, 153–160 (2005).
13) W. Hakamata, M. Muroi, K. Kadokura, T. Nishio, T. Oku, A. Kimura, S. Chiba and A. Takatsuki: Aglycon specificity profiling of α-glucosidases using synthetic probes. *Bioorg. Med. Chem. Lett.*, **15**, 1489–1492 (2005).
14) W. Hakamata, I. Nakanishi, Y. Masuda, T. Shimizu, H. Higuchi, Y. Nakamura, T. Oku, S. Saito, S. Urano, T. Ozawa, N. Ikota, N. Miyata, H. Okuda and K. Fukuhara: Planar catechin analogues with alkyl aide chain, a potent antioxidant and α-glucosidase inhibitor. *J. Am. Chem. Soc.*, **128**, 6524–6525 (2006).
15) J.C. Briggs, A.H. Haines and R.J.K. Taylar: 4-(Sulfonylamino) phenyl α-D-glucopyranoside as competitive inhibitor of yeast α-glucosidase. *J. Chem. Soc. Chem. Commun.*, **18**, 1410–1411 (1993).
16) K. Fukuhara, Y. Naito, Y. Sato, I. Nakanishi and N. Miyata: Generation of oxygen radicals and DNA-cleaving ability in quinone/NADH system. *Magnet. Reson. Med.*, **13**, 139–142 (2002).
17) K. Fukuhara and N. Miyata: Resveratrol as a new type of DNA-cleaving agent. *Bioorg. Med. Chem. Lett.*, **8**, 3187–3192 (1998).
18) K. Fukuhara, M. Nagakawa, I. Nakanishi, K. Ohkubo, K. Imai, S. Urano, S. Fukuzumi, T. Ozawa, N. Ikota, M. Mochizuki, N. Miyata and H. Okuda: Structural basis for DNA-cleaving activity of resveratrol in the presence of Cu(II). *Bioorg. Med. Chem.*, **14**, 1437–1473 (2006).

DNA 切断活性を有する α-グルコシダーゼ阻害剤の設計と合成

袴田 航[1], 山本恵美子[1,2], 室井 誠[3], 望月正隆[2]
栗原正明[1], 奥田晴宏[1], 福原 潔[1]
[1] 国立医薬品食品衛生研究所有機化学部
(158–8501 東京都世田谷区上用賀 1–18–1)
[2] 共立薬科大学薬学部
(105–8512 東京都港区芝公園 1–5–30)
[3] 理化学研究所長田抗生物質研究室
(351–0198 和光市広沢 2–1)

グルコース飢餓，ウイルス感染，低酸素状態などの小胞体ストレスは小胞体に高次構造異常タンパク質を蓄積させる。細胞は分子シャペロンを転写レベルで誘導するunfolded protein response(UPR)を誘起するなどして小胞体ストレスに抵抗するが，強い小胞体ストレスは細胞をアポトーシスへと誘導する。よって小胞体ストレスに起因するアポトーシスをがん細胞で誘導する化合物は抗がん剤となりうる。現在，新規な抗腫瘍薬の一つとして，がん細胞におけるアポトーシス誘導を標的とした抗腫瘍薬の開発が行われている。そこで我々は，*N*-結合型糖鎖プロセッシング酵素を阻害することにより小胞体に高次構造異常タンパク質を蓄積させ，それによる小胞体ストレスによって誘起されるUPRを阻害することによりアポトーシスを誘導する化合物(小分子アポトーシス誘導化合物)としてスルホンエステル誘導体(**1**–**6**)とスルホンアミド誘導体(**7**–**12**)を設計し(Fig. 1)合成を行った(Fig. 3–4)。合成した化合物(**1**–**12**)のα-グルコシダーゼ阻害活性(Table 1)とDNA切断活性(Table 2)について検討を行った。更に，細胞レベルでの*N*-結合型糖鎖プロセッシング酵素阻害活性についても検討した。その結果，ナフチル基を有する化合物**6**と**12**が，*S. cerevisiae*由来α-グルコシダーゼに対しIC_{50}=51.7 μMと74.1 μM，*B. stearothermophilus*由来α-グルコシダーゼに対しIC_{50}=60.1 μMと89.1 μMの阻害活性を示し，化合物**12**が最も強くDNA切断活性を示した。しかし，すべての化合物が細胞レベルにおいて，酵素阻害活性を示さなかった。以上，酵素レベルにおいてα-グルコシダーゼ阻害活性とDNA切断活性を有する小分子を見いだした。今後は，細胞レベルにおいても有効な化合物設計を行う予定である。

J|A|C|S
COMMUNICATIONS

Published on Web 05/03/2006

Planar Catechin Analogues with Alkyl Side Chains: A Potent Antioxidant and an α-Glucosidase Inhibitor

Wataru Hakamata,[†] Ikuo Nakanishi,[‡,§] Yu Masuda,[∥] Takehiko Shimizu,[⊥] Hajime Higuchi,[⊥] Yuriko Nakamura,[#] Shinichi Saito,[#] Shiro Urano,[⊥] Tadatake Oku,[∥] Toshihiko Ozawa,[‡] Nobuo Ikota,[‡] Naoki Miyata,[◇] Haruhiro Okuda,[†] and Kiyoshi Fukuhara*[,†]

Division of Organic Chemistry, National Institute of Health Sciences, Setagaya-ku, Tokyo 158-8501, Japan, Redox Regulation Research Group, Research Center for Radiation Safety, National Institute of Radiological Sciences, Inage-ku, Chiba 263-8555, Japan, Graduate School of Engineering, Osaka University, SORST, Japan Science and Technology Agency, Suita, Osaka 565-0871, Japan, College of Bioresource Sciences, Nihon University, Fujisawa, Kanagawa 1866, Japan, Department of Applied Chemistry, Shibaura Institute of Technology, Minato-ku, Tokyo 108-8548, Japan, Faculty of Science, Tokyo University of Science, Shinjuku-ku, Tokyo 162-8601, Japan, and Graduate School of Pharmaceutical Sciences, Nagoya City University, Mizuho-ku, Nagoya, Aichi 467-8603, Japan

Received November 15, 2005; E-mail: fukuhara@nihs.go.jp

As mitochondrial oxidative damage[1] or oxidative modification of low-density lipoprotein (LDL)[2] contribute significantly to a range of degenerative diseases and further production of reactive oxygen species (ROS), it might be advantageous to develop lipophilic antioxidants which would be able to suppress mitochondrial ROS production or LDL oxidation due to their affinity to lipid particles or membrane. Recently, we synthesized planar catechin analogue (**PC1**), in which the catechol and chroman structure in (+)-catechin are constrained to be planar, by the reaction of (+)-catechin with acetone in the presence of $BF_3 \cdot Et_2O$.[3,4] The rate of hydrogen transfer from **PC1** to galvinoxyl radical (**G**•), a stable oxygen-centered radical, is about 5-fold faster than that of hydrogen transfer from the native (+)-catechin to **G**•. **PC1** also shows an enhanced protective effect against oxidative DNA damage induced by the Fenton reaction without the pro-oxidant effect, which is usually observed in the case of (+)-catechin. We also have found that **PC1**, as well as stilbene resveratrol[5] which is a typical cancer chemopreventive agent present in grapes, inhibits cell growth through induction of apoptosis in cancer cell lines (data not shown). Therefore, we envisioned that a conformationally constrained planar catechin might be valuable in the development of a new type of clinically useful antioxidant, if the hydrophobicity of **PC1** could be controlled so as to fine-tune its membrane binding and penetration into the phospholipid bilayer. Here, we describe a synthetic method for planar catechin analogues (**PCn**), the lipophilicity of which was controlled by changing the length of the alkyl chains. Also described are their remarkable antioxidative potencies and α-glucosidase inhibitory activities.

The synthesis of **PCn** was carried out by reacting catechin with various ketones having alkyl chains of different lengths. However, the previously reported method for the synthesis of **PC1**[3] is inapplicable to other **PCn** synthesis. Because the original reaction is carried out in a solution of acetone, the synthesis of **PCn** is limited to using the corresponding ketone as a solvent. Therefore, it was necessary to improve the synthetic method of **PC1** to be able to introduce various types of ketones into the catechin structure using a synthetic scheme applicable for any **PCn** production. We attempted to optimize the reaction using a combination of various acids and solvents, and finally, it was shown that the reaction using silyl Lewis acids such as TMSOTf, TESOTf, or TBSOTf gave the desired products in high yields. Typically, (+)-catechin and 1.2 equiv of ketone in THF was treated with 1.2 equiv of TMSOTf at −5 °C to form the desired **PCn**. This reaction was used to provide a series of **PC1** ≈ **PC6**, 44−76% yield (Scheme 1), with slightly different lipophilicity.

PCn were evaluated for their radical scavenging activities against DPPH (2,2-di(4-tert-octylphenyl)-1-picrylhydrazyl) radical and AAPH (2,2′-azobis(2-amidinopropane) dihydrochloride)-derived peroxyl radical (Scheme 2). The hydrogen abstraction of **PCn** by DPPH radical in deaerated acetonitrile solution was monitored using the decrease of the visible absorption band at 543 nm due to DPPH radical that obeyed pseudo-first-order kinetics. The second-order rate constant (k_{HT}) for hydrogen abstraction of **PCn** by DPPH radical was then determined (Table 1). Similar to what was found with hydrogen abstraction by galvinoxyl radical,[3] the k_{HT} value (533 M^{-1} s^{-1}) of **PC1** is significantly larger than that of (+)-catechin (305 M^{-1} s^{-1}), indicating that the radical-scavenging activity of catechin using DPPH radical increased due to constraining the (+)-catechin in a planar configuration. In addition, it was found that the larger the number of carbon atoms there were in the alkyl chains, the greater the DPPH radical scavenging rates became, with the k_{HT} value of **PCn** plateauing at $n = 4$. The radical scavenging ability of **PCn** with longer side chains might be attributed to the −I effect of the side chain that stabilizes the cation radical formed after electron transfer from **PCn** to DPPH. The radical scavenging activities of **PCn** in aqueous solution were investigated using AAPH as a source of free radicals in phosphate buffer (Table 1). AAPH-derived peroxyl radicals react with luminol to generate prolonged luminescence,[6] and the antioxidative activities of **PCn** were determined using the concentration of **PCn** where the luminescence is reduced to 50%. As a result, the antioxidative activity of planar catechin in phosphate buffer was again stronger than that of catechin as well as its antioxidative activity in acetonitrile. The alkyl side chains also affect the antioxidative activity; an increase ($n = 1-3$) in the length of the alkyl chains tends to increase the antioxidative activity, with **PC3** showing the strongest antioxidative effect. However, further increase ($n = 4-6$) in the length of the side chain seems to weaken the antioxidative effects, which is consistent with the suggestion that longer alkyl side chains result in the formation of amphiphilic micelles in aqueous solvent.

For the evaluation of lipophilic **PCn** as antioxidants against biomolecular injury caused by ROS, the protecting effect of **PCn** on oxidative DNA damage induced by the Fenton reaction was

† National Institute of Health Sciences, Japan.
‡ National Institute of Radiological Sciences, Japan.
§ Osaka University, SORST, Japan Science and Technology Agency.
∥ Nihon University.
⊥ Shibaura Institute of Technology.
Tokyo University of Science.
◇ Nagoya City University.